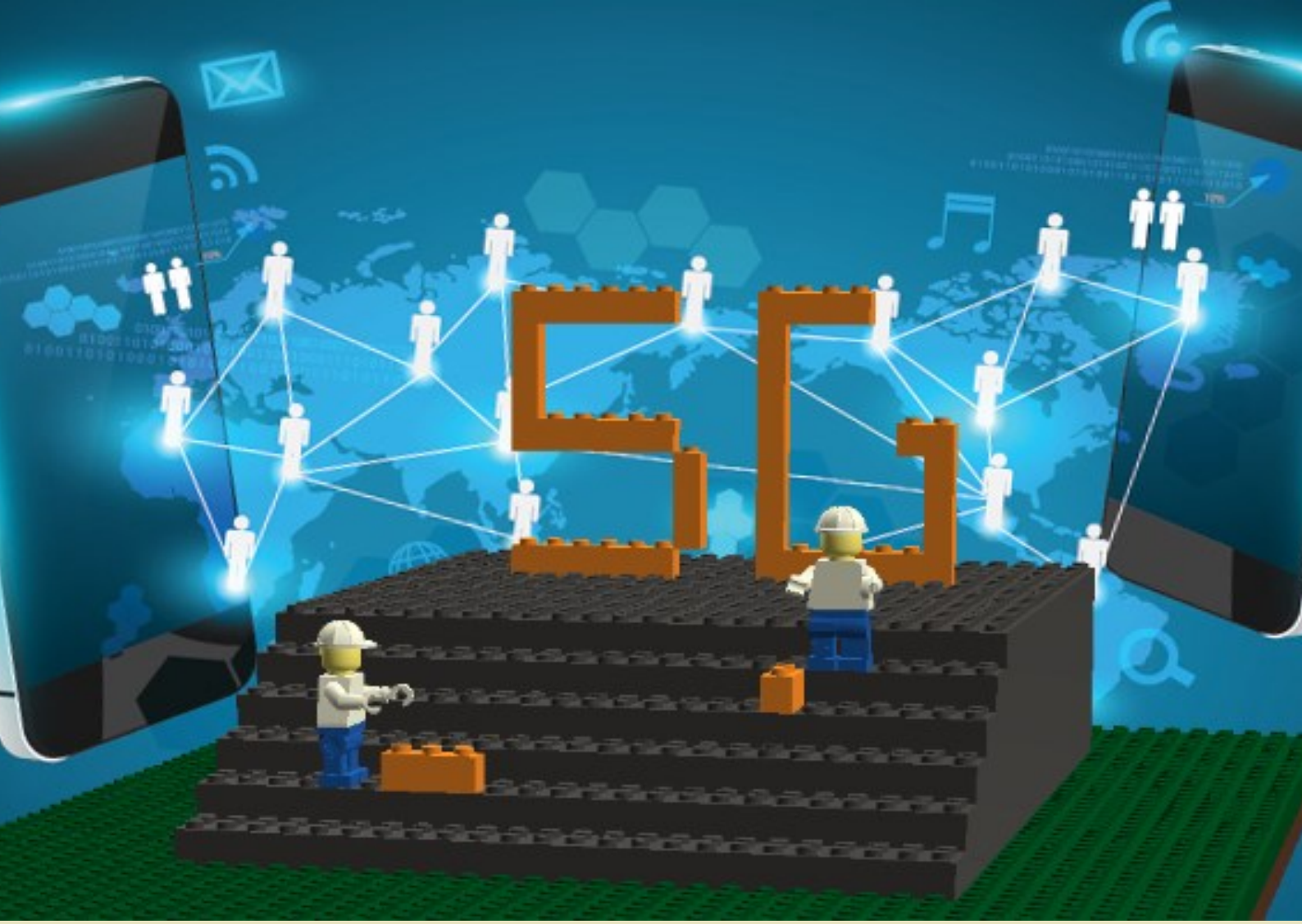

Juliene Monteiro Goenopawiro

NEXT GENERATION MOBILE NETWORK SUPPORTED BY NG-PON2

Dissertation submitted in partial fulfillment of the requirements for the degree of Master of Science in Electrical and Computer Engineering

February 2018

· U C ·

UNIVERSIDADE DE COIMBRA

Source for image background used in front page

https://onlinemarketresearchreports.wordpress.com/2014/12/02/mobile-network-and-device-optimization-market-and-forecasts-2014-2019/

Last visited in February 14th, 2018

Main image[2] created using LEGO Digital Designar 4.3

https://www.lego.com/en-us/ldd

Last visited in February 14th, 2018

• U  C •

FCTUC FACULDADE DE CIÊNCIAS
E TECNOLOGIA
UNIVERSIDADE DE COIMBRA

Department of Electrical and Computer Engineering

Integrated Master in Electrical and Computer Engineering

Next Generation Mobile Network Supported by NG-PON2

Juliene Monteiro Goenopawiro

Examination Committee

President: Professor Henrique José Almeida da Silva, PhD

Member: Professor Teresa Martinez dos Santos Gomes, PhD

Advisor: Professor Maria do Carmo Raposo de Medeiros, PhD

10th March, 2018

Resumo

Esta dissertação aborda o estudo da integração e do suporte da rede móvel de quinta geração, 5G, pela rede de acesso da segunda próxima geração de rede ótica passiva (Next Generation of Passive Optical Networks – NG-PON2). É considerada a arquitetura de rede de acesso rádio centralizada (C-RAN) e a interface comum de rádio pública (CPRI). Novas soluções de rede de acesso móvel são necessárias devido à massificação dos dispositivos móveis e consequente necessidade de maior largura de banda. C-RAN trouxe uma nova dinâmica à rede de acesso móvel com a divisão dos componentes da tradicional estação base (BS) em unidade digital (DU) e unidade de rádio (RU) e com a localização das DUs numa localização central. Esta centralização permite partilha de recursos entre DUs do mesmo Central Office (OC) e permite que essas DUs comuniquem com várias RUs via fronthual que implementa tecnologia de radio sobre fibra (RoF) gerida, por exemplo, pela CPRI. A CPRI apresenta taxa de bits constante cujas opções variam de $614,4$ Mbps referenciada como opção 1 até a opção 10 que é de $24,33$ Gbps. O protocolo CPRI é definido para a camada física e para a camada de ligação. A nova geração de rede móvel, a denominada rede 5G, está a ser estudada de modo a acompanhar o crescimento exponencial de utilizadores móveis e consequentemente a reivindicação acentuada por melhores serviços oferecidos pela rede móvel. A ideia base é a do reaproveitamento de infraestruturas de redes já existentes e uma das soluções para o desenvolvimento da rede 5G baseia-se na convergência da rede móvel e da rede fixa.

A tecnologia de rede de acesso de fibra ótica promissora para esta convergência é a NG-PON2. A NG-PON2 é a primeira PON padronizada a suportar a tecnologia de multiplexação por divisão de comprimento de onda (Wavelength Division Multiplexing – WDM) e tem uma capacidade de transmissão de 40 Gbps e 10 Gps na direção downstream e upstream, respetivamente. O que permite que esta rede seja capaz de suportar tráfego gerado por aplicações que requerem muita largura de banda bem como o tráfego de backhaul

e o de fronthaul de redes móveis. Uma redução nos transreceptores utilizados na rede é possível graças ao conceito de sistema de comprimento de onda agnóstico que consiste na alocação sintonizável de comprimentos de onda na direção upstream, A gestão desta sintonização automática é feita através do canal de controlo auxiliar de gestão (Auxiliary Management Control Channel - AMCC), que para além de transmitir informações de atribuição de comprimento de onda transmite também dados de operação de administração e de gestão. O plano de comprimento de onda do NG-PON2 coexiste com os planos de comprimento de ondas de sistemas PON anteriores como G-PON, XG-PON1 e sobreposição de vídeo de radiofrequência (RF) o que permite reutilização das infraestruturas já existentes. A multiplexação por divisão de tempo e comprimento de onda (TWDM) e a multiplexação por divisão de comprimento de onda ponto-a-ponto (PtP WDM) são duas tecnologias do NG-PON2 e podem ser incorporados na mesma infraestrutura de fibra. O TWDM PON é utilizado para acesso residencial enquanto que o PtP WDM-PON é utilizado para serviços empresariais e para serviços móvel de backhaul e de fronthaul. Cada ONU da PtP WDM PON é servida por um par de comprimentos de onda upstream e downstream e cada par é dedicado a uma ONU. O OLT é responsável pela multiplexação dos comprimentos de onda downstream para uma fibra bidirecional compartilhada. O AMCC é adicionado a cada comprimento de onda individual tanto na direção downstream quanto na direção upstream. Os modos transcodificado e transparente determinam a forma como o conteúdo do AMCC é implementado e transportado através do canal físico. Contudo, este conteúdo, a sinalização AMCC, não depende da forma como é transmitida. No modo transparente, a sinalização AMCC e o sinal de dados CPRI são tratados em paralelo e são adicionados para transporte sendo que a sinalização AMCC é adicionada ao sinal CPRI no mesmo comprimento de onda com a mínima interferência possível por parte da sinalização AMCC no sinal CPRI. Existem três abordagens para a adição da sinalização AMCC no sinal de dados CPRI, por supermodulação de banda base, por esquema de tom piloto e por esquema de supermodulação de fase em cascata.

O foco é a implementação fora de banda usando um tom de radiofrequência (RF). Nesta dissertação foi desenvolvido um modelo de simulação capaz de estudar sistematicamente o efeito do canal AMCC para diferentes parâmetros operacionais quando o transmissor óptico encaminha um laser de feedback distribuído (DFB) seguido de um modulador Mach-Zehnder (MZM).

Abstract

This dissertation addresses aspects of the integration and support of the fifth-generation mobile network, 5G, by the Second Next Generation Passive Optical Networks (NG-PON2) access network, it is focused on the Centralized Radio Access Network architecture (C-RAN) and the Common Public Radio Interface (CPRI). New mobile access network solutions are needed due to the massification of mobile devices and consequent demand for greater bandwidth. C-RAN has brought a new dynamic to the mobile access network with the division of the components of the traditional base station (BS) into digital unit (DU) and radio unit (RU) and the delocalization of the DUs to a central point. This centralization allows resource sharing between DUs of the same Central Office (OC) and allows these DUs to communicate with several RUs via a fronthaul that is implemented on radio over fiber (RoF) technology though, for example, CPRI. CPRI has a constant bit rate whose options range from 614.4 Mbps referenced as option 1 to option 10 which is 24.33 Gbps. The CPRI protocol is defined in the physical layer and in the connection layer. The new generation of mobile network, the so-called 5G network, is being studied and deployed to keep up with the exponential growth of mobile users and consequently the increased demand for better services offered by the mobile network. The basic idea is to reuse existing network infrastructures and one of the solutions for the development of the 5G network is based on the convergence of the mobile network and the fixed network.

The promising fiber optic access network technology for this convergence is the NG-PON2. NG-PON2 is the first PON standard to support Wavelength Division Multiplexing (WDM) technology and has a 40 Gbps and 10 Gbps transmission capacity in the downstream and upstream direction, respectively. This allows this network to be able to handle traffic generated by bandwidth-intensive applications as well as backhaul and fronthaul traffic from mobile networks. A reduction in the transceivers used in the network is possible thanks to the concept of agnostic wavelength system which consists of

the tunable allocation of wavelengths in the upstream direction. The management of this automatic tuning is done through the Auxiliary Management Control Channel (AMCC), which in addition to transmitting wavelength assignment information also transmits administration and management data. The wavelength plane of the NG-PON2 coexists with the wavelength planes of previous PON systems such as G-PON, XG-PON1 and overlapping of radio frequency (RF) video, which allows reuse of existing infrastructures. Time-wavelength-division multiplexing (TWDM) and point-to-point wavelength division multiplexing (PtP WDM) are two technologies of NG-PON2 and can be incorporated into the same fiber infrastructure. The TWDM-PON is used for residential access while the PtP WDM-PON is used for business services and for backhaul and fronthaul mobile services. Each PtP WDM-PON ONU is served by a pair of upstream and downstream wavelengths and each pair is dedicated to one ONU. The OLT is responsible for the multiplexing of the downstream wavelengths for a shared bidirectional fiber. AMCC is added to each individual wavelength in both downstream and upstream directions. Transcoded and transparent modes determine how AMCC content is implemented and transported across the physical channel. However, this content, AMCC signaling, does not depend on how it is transmitted. In the transparent mode, AMCC signaling and CPRI data signal are treated in parallel and are added for transport where AMCC signaling is added to the CPRI data signal at the same wavelength with the least possible interference by signaling in the signal data. There are three approaches to adding AMCC signaling to the CPRI data signal, by base-band supermodulation, by pilot tone scheme, and by cascade phase supermodulation scheme.

The focus is on out-of-band implementation using a radio frequency (RF) tone. In this dissertation we develop a simulation model able to study systematically the effect of the AMCC channel for diferent operational parameters when the optical transmitter consists of a Distributed Feedback (DFB) laser followed by a Mach-Zehnder Modulator (MZM).

Acknowledgments

More than obtaining the Master's degree in Electrical Engineering and Computers this dissertation represents the culmination of my stay in Coimbra, which began at the moment of enrollment in the course and lead me to embrace the experiences of my newest city.

That is why I begin by thanking my advisor, Maria do Carmo Medeiros, for accepting my application for a dissertation even though I would be residing in the Netherlands, which would mean that we both work in different countries. I acknowledge the availability of the professor to communicate through e-mails and to have meetings via Skype calls to guide me and to indicate me papers which covered a good area of study for the accomplishment of the dissertation. From our face-to-face meetings I emphasize the professor's dedication to explaining me so I can understand, for example, the reason for a particular implementation, and the professor's sympathy and goodwill. I am also grateful for the fact that the professor continued to guide me even though she was on her sabbatical, which sensitized me a lot.

Regarding contributions in the dissertation, I thank Dr. Paulo Almeida for the assignment of the MATLAB® model of the continuous laser used in this dissertation and to Beatriz Manata for providing me the text document of her dissertation to serve as an example of proper formatting and for assisting me in the ORCID Identifier[1] register and with the Creative Commons Licence [2]. I also thank the members of the jury, Professor Teresa Martinez and Professor Henrique Silva, for enabling the date of the defense to be at a suitable time for all constituents of the jury.

To the DEEC[3] professors, I am eternally grateful for their kind gestures of help. To Professor Teresa Martinez and Professor Lúcia Martins for making me feel welcome to a

[1] `https://orcid.org/node/8`
[2] `https://creativecommons.org/licenses/`
[3] Departamento de Engenharia Eletrotécnica e de Computadores

new reality in a new country, and her cordiality over the years. To Professor Jorge Lobo for the opportunity granted to the students of the 3rd phase, which was my case since I was only able to enroll in the course in November, to take a practical test even though the date of its completion had expired. To Professor Luiz de Sá for his commitment in explaining to the students until they fully grasp the subject. To Professor Silverinha for his different approach in teaching and for being an impartial professor. To Professor Rita Silva for her willingness to ask questions. To Professor Marco Gomes for his concern for the delivery of a work of mine. To Professor Henrique Silva for gracefully allowing me to attend the STO[4] subject in the last academic year without compulsory presence and to be able to send the exercises solved by email. And to all the teachers who in one way or another contributed to my academic progress.

My thanks also go to my colleagues for the sharing of "sebenta"/notes and for getting along with them in this Coimbra that is well known for its tradition and idoneity as it is sung in the song: "Coimbra é uma lição/ De sonho e tradição".

To Escola Amor de Deus, especially to teachers, for providing me with the bases required in this academic course. To Sister Francisca for her affection, guidance and for her "those who do not study do not fail principle.".

To the APCC[5] which was until 2016 my source of smiles and hugs of the week as well as a way for me to recharge my energy levels. For making me come out of my bubble of distorted reality and for the consequent improvement of my five senses in attention to others. To the misses[6] who adopted me as a younger sister and introduced me to the community where I had enriching experiences. To SPES[7] for teaching me to "Ser capaz de mais/ Poder sonhar, poder sorrir". To the Instituto Justiça e Paz for all affection from the staff of the house groups.

To my friends for always being present at the appropriate time and for accepting my "brukutu" way of being. To Benny and the girls of the house, where one does not enter with the "brebidom" because there is no "terpida", because they received me so well and

[4]Sistemas de Transmissão Óticos
[5]Associação de Paralisia Cerebral de Coimbra
[6]Missionárias Servidores do Evangelho da Misericórdia de Deus
[7]Serviço Pastoral do Ensino Superior

for providing me with a place to sleep so that I could stay in Coimbra for the last few weeks. To Filhota, especially for "quebrar-me o galho" (helping me out) on February 11th. To Helen for accepting my last-minute request to correct the English of the present document.

To Diogo for making me re-believe in fairy tales and that there is always a white horse prince for a lost princess. And particularly in recent weeks for being my personal assistant with the task of reviewing and dealing with the details of this document.

To my family, especially Mamá Titi, my mother and Toi, who with little helped me to complete this academic path. To Tio, Tia, Nuno, Bea, and Milo for being my safe harbor in Coimbra and for everything they did for me. To Papá Té for the love that I am still feeling which made me grow and be who I am today. To "os trapalhões" because they are my "irmãos do peito" (soul brothers) and my source of encouragement. To uncle Nelito who always believed in me. To aunt Rosa and uncle Duarte who usually telephoned to know how I was. To aunt Salome who was always worried about me and when she had some extra cash she would recharge my balance on my cell phone so that I would be able to communicate. To Nadine for making me laugh. To my half-sisters for the good times we spent. To my father and his family for friendship and encouragement. And to Diogo's parents for making their apartment in Furadouro available to me so that I had a place to stay when I was in Portugal.

To all of you who during these years have guided me with your advice and encouraged me with your words and attitudes, my sincere thanks!

I also thank the obstacles that I have encountered along the way and that I have been learning to overcome. These have brought valuable lessons to my life.

And with a full heart, I start another path in tune with the famous phrase of our poet Eugénio Tavares: "Si ka badu, ka ta biradu".

Juliene

Contents

List of Acronyms

1G	First generation of mobile network
2G	Second generation of mobile network
3G	Third generation of mobile network
3GPP	3rd Generation Partnership Project
4G	Fourth generation of mobile network
5G	Fifth generation of mobile network
AMCC	Auxiliary Management and Control Channel
APON	Asynchronous Transfer Mode Passive Optical Network
ATM	Asynchronous Transfer Mode
AxC	Antenna-carrier
BBU	Baseband Unit
BER	Bit Error Ratio
BPON	Broadband Passive Optical Network
BS	Base Station
C&M	Control and Management
C-RAN	Centralized Radio Access Network
CBR	Constant Bit Rate
CDMA	Code Division Multiple Access
CO	Central Office

CPRI	Common Public Radio Interface
CW	Control Word
D-RoF	Digital Radio over Fiber
D/S	DownStream
DFB	Distributed Feedback
DL	DownLink
DU	Digital Unit
E-UTRA	Evolved Universal Terrestrial Radio Access
EDGE	Enhanced Data Rates for GSM Evolution
EPON	Ethernet Passive Optical Network
ETSI	European Telecommunications Standards Institute
FDD	Frequency Division Duplex
FDMA	Frequency Division Multiple Access
FEC	Forward Error Correction
FSAN	Full-Service Access Network
FTTH	Fiber-To-The-Home
GE	Gigabit Ethernet
GPON	Gigabit Passive Optical Network
GPRS	Generalized Packet Radio Service
GSM	Global System for Mobile communications
HDLC	High level Data Link Control
HSDPA	High-Speed Downlink Packet Access
HSPA	High-Speed Packet Access
HSUPA	High-Speed Uplink Packet Access

I	In-phase
IEEE	Institute of Electrical and Electronics Engineers
IMT	International Mobile Telecommunication
IQ	In-phase and Quadrature-phase
ISG	Industry Specification Group
ITU	International Telecommunication Union Telecommunication
ITU-T	International Telecommunication Union
LTE	Long-Term Evolution
MFH	Mobile Fronthaul
MIMO	Multiple Input Multiple Output
MNO	Mobile Network Operator
MZM	Mach-Zehnder Modulator
NG-PON	Next Generation Passive Optical Network
NG-PON1	First Next Generation Passive Optical Network
NG-PON2	Second Next Generation Passive Optical Network
NGMN	Next Generation Mobile Network
OBSAI	Open Base Station Architecture Initiative
ODN	Optical Distribution Network
OFDM	Orthogonal Frequency Division Multiplexing
OFDMA	Orthogonal Frequency Division Multiple Access
OLT	Optical Line Terminal
OLT-CT	Optical Line Terminal-Channel Termination
ONU	Optical Network Unit
ORI	Open Radio Interface

PMD	Physical Media Dependent
PON	Passive Optical Network
PRBS	PseudoRandom Binary Sequence
PT	Pilot Tone
PtMP	Point-to-MultiPoint
PtP	Point-to-Point
Q	Quadrature-phase
RAN	Radio Access Network
RE	Radio Equipment
REC	Radio Equipment Control
RF	Radio Frequency
RoF	Radio over Fiber
Rp3	Reference Point 3
RRH	Remote Radio Heads
RU	Radio Unit
SFP	Small Form-factor Pluggable
SMF	Single Mode Fiber
TC	Transmission Convergence
TDD	Time Division Duplex
TDM	Time Division Multiplexing
TDM PON	Time Division Multiplexing Passive Optical Network
TDMA	Time Division Multiple Access
TWDM	Time Wavelength Division Multiplexing
U-Plane	User Plane

U/S	UpStream
UL	UpLink
UMTS	Universal Mobile Telecommunication System
UTRA	Universal Terrestrial Radio Access
UTRAN	Universal Terrestrial Radio Access Network
WDM	Wavelength Division Multiplexing
WDM PON	Wavelength Division Multiplexing Passive Optical Network
WiMAX	Worldwide Interoperability for Microwave Access
WM	Wavelength Multiplexer
XG-PON1	Asymmetric 10 gigabit capable Passive Optical Network
XG-PON2	Symmetric 10 gigabit capable Passive Optical Network

List of Figures

List of Tables

Chapter 1

Introduction

Chapter 1 dedicates to the presentation of the work plan of this dissertation in which the motivation, the contextualization and the objectives are presented in sections 1.1, 1.2 and 1.3 respectively. In section 1.4, the structure of the document is described and the final section, 1.5, indicates the contributions of this work.

1.1 Motivation

Nowadays it is possible to access the Internet anywhere and anytime through mobile devices like smartphones, tablets, or even small gadgets and appliances that connect to the Internet, the Internet of Things (IoT). It is common to respond emails while we are on the bus on our way to work, entertain ourselves with online videos while we are in the dentist's waiting room, listen to music streaming while running in the park or publish a photo of a landscape on a social network while we are on vacation.

This scenario can be verified by the results of the survey conducted in 2016 on Information and Communication Technologies (ICT) usage in households and by individuals [1] issued by Eurostat, the statistical office of the European Union[1]. It states that: "More than 80% of persons aged 16 to 74 in the European Union used the internet in 2016, in many cases via several different devices. Mobile phones or smart phones were the device most used to surf the internet, by over three-quarters (79%) of internet users. They were followed by laptops or netbooks (64%), desktop computers (54%) and tablet computers (44%)." The results of "Main devices used in the European Union to surf the internet, by age groups (as % of internet users over the last three months)" is represented in figure 1.1.

[1] `http://ec.europa.eu/eurostat`

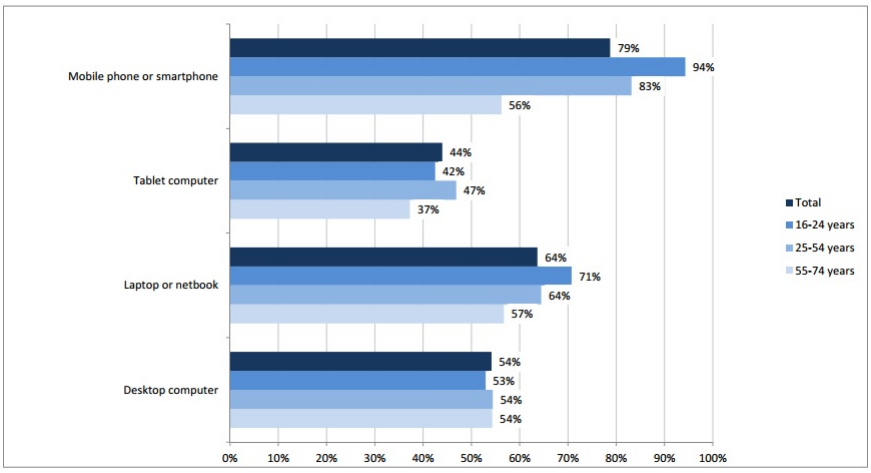

Figure 1.1: Main devices used in 2016 to surf the internet.
Source: Eurostat, the statistical office of the European Union [1]

This reality is possible thanks to the deployments of fourth generation (4G) of mobile networks which provides reasonable rates of transmission to the mobile customers to use the Internet. And thanks to the mobile modem that allows laptops and netbooks to connect to the mobile network.

With all these devices connected in the mobile network to use the Internet, the traffic has been growing exponentially. To be aware of the impact of this mobile devices on the mobile traffic, according to a study presented by Cisco and/or its affiliates in [2] "**Global mobile data traffic grew 63 percent in 2016.** Global mobile data traffic reached 7.2 exabytes per month at the end of 2016, up from 4.4 exabytes per month at the end of 2015. (One exabyte is equivalent to one billion gigabytes, and one thousand petabytes.) **Mobile data traffic has grown 18-fold over the past 5 years.** Mobile networks carried 400 petabytes per month in 2011." And the trend is the mobile traffic continues to increase as predicted in [2] which states that "**Global mobile data traffic will increase sevenfold between 2016 and 2021.** Mobile data traffic will grow at a compound annual growth rate (CAGR) of 47 percent from 2016 to 2021, reaching 49.0 exabytes per month by 2021." As we can see in figure 1.2 representing "Cisco Forecasts 49 Exabytes per Month of Mobile Data Traffic by 2021".

The current mobile devices are so versatile that in addition to surf the Internet via the mobile network, these devices can also access the Internet by connecting to the fixed network through their fixed wireless (Wi-Fi) interface. As reported by [2]: "Mobile offload

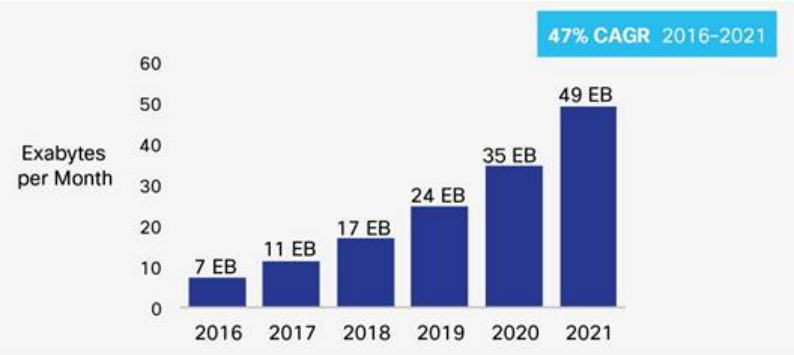

Figure 1.2: Cisco Forecasts 49 Exabytes per Month of Mobile Data Traffic by 2021
Source: Cisco VNI Mobile, 2017 [2]

exceeded cellular traffic by a significant margin in 2016. Sixty percent of total mobile data traffic was offloaded onto the fixed network through Wi-Fi or femtocell in 2016. In total, 10.7 exabytes of mobile data traffic were offloaded onto the fixed network each month." A representation of mobile versatility in access internet is illustrated in figure 1.3.

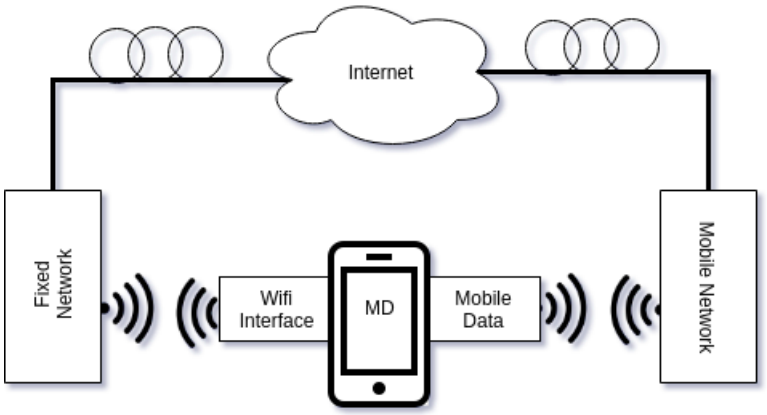

Figure 1.3: Current access to internet though a mobile device (MD)

The total mobile data traffic is generated by the traditional online applications and by the new applications such as HDTV, 3D-TV, video services, cloud computing, tele-conferencing, multi-player HD video games, VoIPX, and P2PX. These new applications have dominated the Internet and today these applications are the applications of choice for customers. Relative to video streaming, the study presented in [2] informs "**Mobile video traffic accounted for 60 percent of total mobile data traffic in 2016.** Mobile video traffic now accounts for more than half of all mobile data traffic."

As we see, a new paradigm in the telecommunications network is emerging. The willingness of users to use a Wi-Fi interface on their mobile device, and the video streaming

is diminishing the difference between fixed and mobile access in terms of usage as indicate in [3]. Furthermore, the requirement for capacity enhancement to satisfy the traffic needs has led to the development of new approaches and standards. A promising approach is to mutualize the telecom operator's access infrastructure to allow the most efficient use of network resources, and consequently a better fixed-mobile convergence and an increase of network capacity.

1.2 Context

"Fixed and mobile networks themselves have been optimized and have evolved independently from each other" transcribed from [3]. From one side, the fiber optic access network is massively installed in the metropolitan area, arriving to the customers homes through the Fiber-To-The-Home (FTTH) technology. With this impressive deployment of FTTH networks plus the Gigabit Passive Optical Networks (GPON) and Gigabit Ethernet (GE) technologies, it is possible to allow high transmission rates at competitive prices thanks to the high bandwidth provided by optical fiber.

From the other side, the architecture of wireless and mobile networks is evolving towards an increase in cell density with the many small cells deployment on a macro cell in the urban areas. To decrease the network costs, the expensive and high-power traditional base stations was evolved to remote radio units. This new architecture, called Centralized Radio Access Network (C-RAN), improves transmission performance by been capable to support the coordination of multiple cells from one central unit.

C-RAN brought a new element in the mobile network: the fronthaul, which is the segment between the remote radio units and the central unit. The fronthaul uses a Digital Radio over Fiber interface (D-RoF), as the Common Public Radio Interface (CPRI), to define the specifications of the radio signal scanning.

According to [8], the Wavelength Division Multiplexing (WDM) PON system has been defined for fronthaul to provide high capacity and low latency, and consequently reducing the number of fibers needed to accommodate the many small cells. This system allows semi-statically assignment of the wavelengths to small cells depending on the mobile traffic

load. As stated in [9], such process is called wavelength tunability and is implemented in WDM PON by an out-of-band control channel denominated as Auxiliary Management and Control Channel (AMCC) which was indicated in [4]. In addition to managing these wavelengths, AMCC also transports control information for data monitoring and other management relevant information that can reduce the number of transceivers used in the network.

WDM PON is one of the technology included in the Second Next Generation of Passive Optical Networks (NG-PON2) standard. NG-PON2 focus on maximum reuse of existing network resources and provides full convergence for all fixed and mobile services by organizing the convergence infrastructure around a main central unit and rationalizing the fiber deployed for FTTH networks.

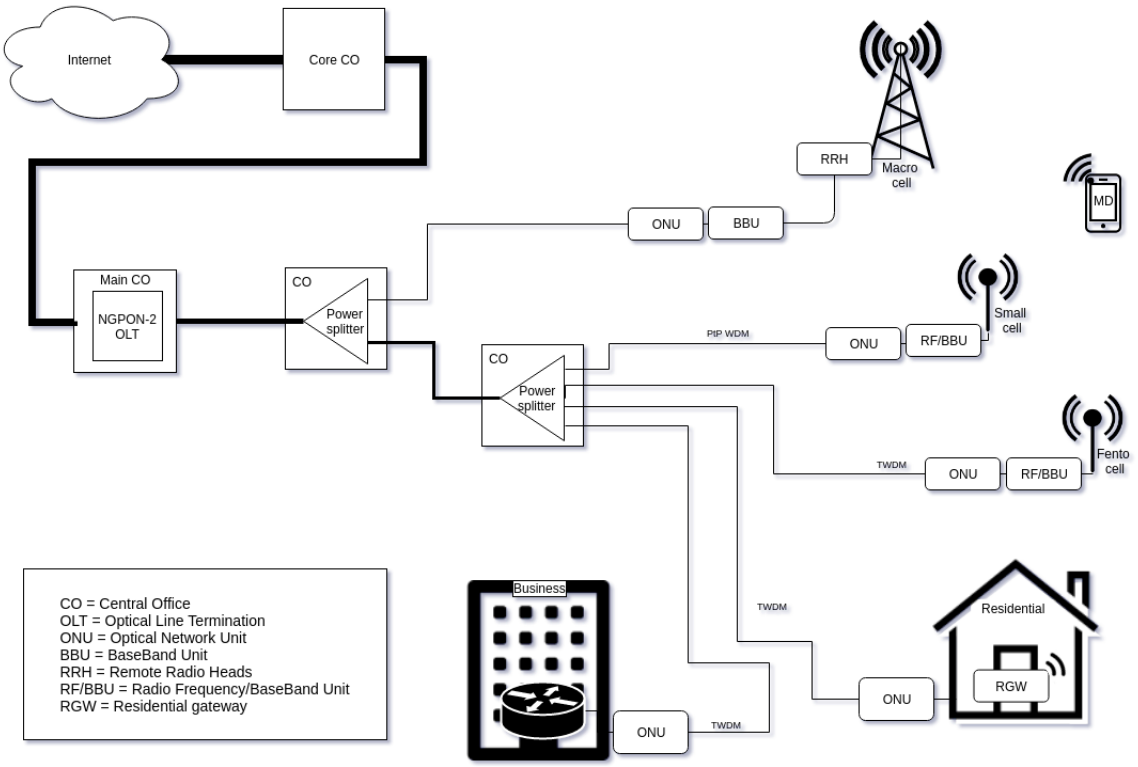

Figure 1.4: Backhaul implementation in an NG-PON2-based converged access architecture. Figure adapted from [3]

The NG-PON2-Based Converged Access with Point-to-Point (PtP) WDM was presented in [3] as one of the methods for pooling access infrastructure. This convergence solution connects base stations, small cells, and fixed access links. The radio remote units from C-RAN are supported on CPRI carried over WDM. And each of the mobile network sites is dynamically assigned a pair of available wavelengths in the NG-PON2 spectrum, in the WDM PON logic. This convergence solution combines PtP WDM overlay channels with

Time Wavelength Division Multiplexing (TWDM) PON. An example of this convergence solution is ilustrated in figure 1.4.

1.3 Objectives

The objective of this dissertation is the study of the integration and support of the fifth generation (5G) of mobile network through the access network NG-PON2. In a first phase, the proposed network architecture is studied. This includes the study of NG-PON2, particularly the mobile network support mechanisms, the study of C-RAN architectures and CPRI. After, to study real implementations of the proposed approach, the work focus on the analysis of the effect of the AMCC on the transmission of CPRI signals from the mobile network.

1.4 Dissertation structure

The remainder of this document thus considers the contributions of this work in section 1.5 and the principal topics are explored the following 6 chapters. The Passive Optical Network is discussed in chapter 2, where the NG-PON2 network was distinguished by the fact of providing high bandwidth and by its key feature of being able to implement a tunable transceiver which allows tunable wavelengths. These tunable wavelengths are controlled and monitored by the AMCC. In chapter 3, the Mobile Network is reviewed, highlighting the C-RAN architecture which allows a better use of infrastructures in the scenario of small cell densification. Fronthaul was introduced with the implementation of C-RAN and is governed by Radio over Fiber (RoF) technology. The RoF technology that is most used is the CPRI whose study was done in chapter 4. In chapter 5 a research on AMCC was carried out to see what has been done so far. In one hand this research refers to the state of the art about the mobile network of the next generation and in the other hand to the state of the art about the control channel itself. In chapter 6, a Case study about the next generation mobile network (NGMN) was carried out by simulation tests, where the simulation results and respective discussions are presented. Finally, a conclusion about the work is made in chapter 7, with a presentation about the principals conclusions and a possible future works in this context.

1.5 Contributions

A survey of works whose subjects of study was the fixed network, the mobile network, and the convergence of these two networks were made. The result of this survey was a compilation of proposed and evaluated solutions of how the mobile network can be supported by the fixed network, more specifically NG-PON2 and C-RAN networks. So, this dissertation provides an overall overview on how mobile networks can be supported by NG-PON2, within the concept of Centralized Radio Access Network.

The key point for this convergence is the concept of agnostic wavelength systems whose wavelengths are tuned thanks to AMCC management. Various experiments were carried out to evaluate the performance of the system by introducing this control channel into the data signals and the results were satisfactory. In this line, a case study was simulated in MATLAB® in order to analyze the impact of the AMCC implementation as a pilot tone (PT) on the CPRI data signal. In what resulted in a MATLAB® program that calculates the BER of the CPRI data signal and the BER of the AMCC signaling channel.

Chapter 2

Passive optical access network

Chapter 2 presents a PON study with section 2.1 describing a brief overview of the current use of the respective network, while in section 2.2 the technical details of the network as well as the evolution of the network are discussed. The NG-PON2 is described in section 2.3 and, lastly, the AMCC is characterized in section 2.4.

2.1 Overview

Currently the fiber optic access network is massively installed, reaching customers homes via FTTH, which can provide Internet access rates in the range of gigabits per second (Gbps) . In Portugal, the download and upload transmission speeds available to consumers, which depends on the service package chosen by them, vary from 100 Megabit per second (Mbps) to 200 Mbps and from 10 Mbps to 20 Mbps respectively. However, very recently some telecom operators have made available service packs with download rates of 1 Gbps and upload rate of 100 Mbps or 200 Mbps[1].

FTTH access technology directly links the Central Office (CO) of a telecommunications operator to a home through a fiber optic network. The fiber reaches the boundary of the residence and from there the signal can be transported to the entire space of the residence through a network using fiber optic, Ethernet network cable, coaxial cable, or wireless communication. Fiber optic cables can carry data at high speeds up to long distances. Optical

[1]Last visited in February 14th, 2018
https://www.meo.pt/pacotes/mais-pacotes/fibra
http://www.nos.pt/particulares/pacotes/todos-os-pacotes/Paginas/pacotes.aspx
http://www.nowo.pt/pdf/NOWO_tarifario.pdf
https://www.vodafone.pt/main/particulares/tv-net-voz/pacotes/

distribution of CO to households is done through direct fiber or shared fiber. The fiber-optic optical distribution network is the cheapest and most popular option. Two competing technologies perform the division of the fiber: Active Optical Networks and PONs.

2.2 Passive Optical Network

PON is described in [10] as "a set of technologies originally created by the Full-Service Access Network (FSAN) working group and standardized by International Telecommunication Union Telecommunication (ITU-T) Standardization group and Institute of Electrical and Electronics Engineers (IEEE). PON is a converged infrastructure that can carry multiple services such as plain old telephone service, voice over IP, data, video, and/or telemetry, in that these services are converted and encapsulated in a single packet type for transmission over the PON fiber." This access system affords low cost, simple maintenance operation, and high-bandwidth provision for the telecommunication operators as indicated in [11].

Defining by [4], a PON is constituted by three main parts, where the bidirectional data transmission takes place, which are: optical line terminal (OLT), optical network unit (ONU), and optical distribution network (ODN). The OLT is located at the service provider's central office, and its main function is to provide the interface between PON and the backbone network which is connected to the core network. The ONU is located at the user terminal, and it provides the service interface to end users. The ODN is the common element of the OLT and the ONU. It is located between OLT and ONU connecting them by using optical fibers and splitters. The ODN usually forms a tree structure with the OLT as the root of the tree and ONUs as the branches or leaves of the tree and works as data distributed device from/to an OLT and ONUs. A representation of PON constituents is shown in figure 2.1.

The PON technologies are classified depending on the data multiplexing scheme. There are three major PON technologies: orthogonal frequency division multiplexing (OFDM) PON, time division multiplexing (TDM) PON, and WDM PON. OFDM PON transmit traffic from/to ONUs by employing several orthogonal subcarriers. TDM PON uses TDM multiplexing in traffic from/to multiple ONU for transmission at upstream/downstream wavelength. WDM PON provides bandwidth to ONUs using multiple wavelengths.

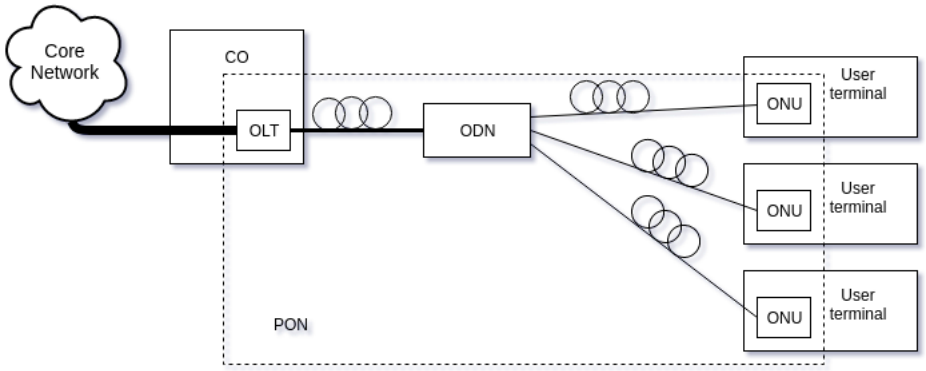

Figure 2.1: A PON is constituted by three main parts

2.2.1 PON evolution

Over the last decades, the PON has evolved considerably. According to [10], [12] and [13], the data rate started from few Mbps in 1995 up till multiple Gbps nowadays, and it will continue to increase in the future. The currently deployed PON networks are TDM PON systems, which have been standardized from 1995 to 2013. WDM PON was first proposed in 1986, and in 2006 WDM PON has already been deployed in Korea. However, due to its high costs the deployment of WDM PON in other countries has been stalled until 2010 when FSAN started investigation of optical access technologies beyond 10 Gbps. This project became known as NG-PON2, and in March 2013 the General Requirements was approved. The series was completed and approved in November 2015. OFDM PON has received intensive research attention in recent years owing to its high bandwidth provisioning. With the WDM or OFDM technology, these PONs are potentially able to provide higher than 40 Gbps data rate and even Tbps data rate. Both WDM PON and OFDM PON are considered as future PON technologies. The only technologies standards until now is the TDM PON and the WDM PON as we can see in the table 2.1, which resumes the evolution of the PON standards.

Asynchronous Transfer Mode (ATM) PON (APON), Broadband PON (BPON), Ethernet PON (EPON), GPON, 10G EPON, and Next Generation PON (NG-PON) are TDM PON technologies and each of these technologies offer different data rates. APON/BPON, GPON, and NG-PON architectures were standardized by the FSAN. Since most telecommunications operators have heavily invested in providing legacy TDM services, these PON architectures are optimized for TDM traffic and rely on framing structures with very strict timing and synchronization requirements. While EPON and 10G-EPON are standardized by the IEEE 802 study group. They focus on preserving the architectural model of Ethernet. No explicit framing structure exists in EPON, and Ethernet frames

<table>
<tr><th rowspan="2">Year</th><th colspan="4">STANDARD (Network downstream/upstream)</th><th rowspan="2">Technology</th></tr>
<tr><th colspan="3">FSAN/ITU-T</th><th>IEEE</th></tr>
<tr><td>1995</td><td colspan="3">ITU-T Recommendation G.957</td><td></td><td></td></tr>
<tr><td>1996</td><td colspan="3">ITU-T Recommendation G.671
ITU-T Recommendation G.982</td><td></td><td></td></tr>
<tr><td>1997</td><td colspan="3">ITU-T Recommendation G.652</td><td></td><td></td></tr>
<tr><td>1998</td><td colspan="2" rowspan="3">G.983.1-2
(APON 155M/155M)</td><td></td><td></td><td rowspan="3">TDM-PON</td></tr>
<tr><td>1999</td><td></td><td></td></tr>
<tr><td>2000</td><td></td><td></td></tr>
<tr><td>2001</td><td rowspan="2">G.983.3-5
(BPON 625M/155M)</td><td rowspan="4">G.983 series
amendments
(APON/BPON)</td><td></td><td rowspan="3">IEEE 802.3ah
(1G-EPON 1G/1G)</td><td rowspan="2">TDM-PON</td></tr>
<tr><td>2002</td><td></td></tr>
<tr><td>2003</td><td></td><td rowspan="3">G.984.1-4
(G-PON 2.5G/1.25G)</td><td rowspan="8">TDM-PON</td></tr>
<tr><td>2004</td><td></td></tr>
<tr><td>2005</td><td></td><td rowspan="6">G.984 series
amendments
(G-PON 2.5G/1.25G)</td><td></td></tr>
<tr><td>2006</td><td></td><td></td><td></td></tr>
<tr><td>2007</td><td rowspan="5">G.984.5-7
(G-PON 2.5G/1.25)</td><td></td><td rowspan="3">IEEE 802.3av
(10G-EPON
10G/1G & 10G/10G)</td></tr>
<tr><td>2008</td><td></td></tr>
<tr><td>2009</td><td></td></tr>
<tr><td>2010</td><td rowspan="3">G.987 series
(XG-PON 10G/2.5G)</td><td></td></tr>
<tr><td>2011</td><td></td><td></td></tr>
<tr><td>2012</td><td></td><td></td></tr>
<tr><td>2013</td><td colspan="2" rowspan="3">G.989 series
(NG-PON2 40G/10G)</td><td></td><td></td><td rowspan="5">WDM-PON</td></tr>
<tr><td>2014</td><td></td><td></td></tr>
<tr><td>2015</td><td rowspan="3">G.989 series
amendments
(NG-PON2 40G/10G)</td><td></td></tr>
<tr><td>2016</td><td></td><td></td><td></td></tr>
<tr><td>2017</td><td></td><td></td><td></td></tr>
</table>

Table 2.1: PON standards

are transmitted in bursts with a standard inter-frame spacing. EPON is defined in IEEE 802.3ah standard and provides 1 Gbps symmetric data rate. 10G EPON is defined in IEEE 802.3av standard and supports both symmetric 10 Gbps downstream and upstream, and asymmetric 10 Gbps downstream and 1 Gbps upstream data rates.

APON is the initial PON specifications defined by the FSAN committee in ITU-T G.983 series [12]. The downstream transmission is a continuous ATM stream at a bit rate of 155.52Mbps or 622.8Mbps. Upstream transmission is in the form of bursts of ATM cells. The upstream channel is divided into 53 slots of 56 bytes at 155.520Mbps, while

the downstream cell stream is divided into frames of 56 cells at 155.520Mbps. BPON, as defined in ITU-T G.983 series [12], is a further improvement of the APON system. With the objective of achieving early and cost-effective deployment of broadband optical access systems, BPON offers numerous broadband services including ATM, Ethernet access, and video distribution.

GPON is specified in ITU-T G.984 series [12]. GPON supports various bit rate options using the same protocol, including a symmetrical data rate of 622 Mbps in both downstream and upstream, a symmetrical data rate of 1.244 Gbps in both streams, as well as a data rate of 2.488 Gbps in downstream and a data rate of 1.244 Gbps in upstream. The data rates supported by typical GPON systems are 2.488 Gbps of downstream bandwidth and 1.244 Gbps of upstream bandwidth. GPON supports full-service including voice, TDM, Ethernet, ATM, leased lines, and wireless extension. GPON also supports radio frequency (RF) video transmission in the waveband from 1.550 to 1.560 nm.

NG-PON is divided into two phases: NG-PON1 and NG-PON2. NG-PON1 focuses on PON technologies that are compatible with GPON standards, as well as the current ODN. While NG-PON2 provides an independent PON system, without being constrained by the GPON standards and the currently deployed outside plant. NG-PON1 is standardized in ITU-T G.987 series [12], and it specifies both asymmetric and symmetric 10G-PONs. The asymmetric 10G-PON is referred as XG-PON1, and it provides the downstream data rate of 9.95328 Gbps and the upstream data rate of 2.48832 Gbps. The symmetric 10G-PON is referred as XG-PON2 and it achieves 10 Gbps in both upstream and downstream.

Regarding to WDM PON, [11] states that this architecture provides higher bandwidth per ONU, low splitting loss, high security, high scalability, and maximum link reach over traditional PONs. WDM PON is a FTTH solution based on a PtP link between the OLT and each ONU, where each subscribers of these ONUs are supplied by a dedicated wavelength. This PtP link is one of the characteristics that differs WDM PON from TDM PON in that the latter implements point-to-multipoint (PtMP) architecture instead. That is, TDM PON shares wavelengths between 32 or even more subscribers, as indicated in [10], whereas WDM PON provides a wavelength for each subscriber. These one or more wavelengths dedicated to one user allow this user to access the full bandwidth accommodated by the wavelengths, and due the fact that the user home only receives its

own wavelength the WDM PON provide superior security and scalability than TDM PON. Another advantage, is that WDM PON allows maximum flexibility and pay-as-you-grow upgrades due the fact that each PtP link run at a different speed and with a different protocol. The WDM multiplexer or de-multiplexer used to send wavelength channel from/to OLT to/from ONU implement filtration technologies as thin film filters, fiber bragg gratings, and array waveguides, whereas TDM-PON use passive splitter.

Due to the WDM PON PtP link, the OLT that supports 32 ONUs must transmit on no less than 32 different wavelengths, and each ONU should supports all wavelength channels and operate at their own wavelengths. Therefore, several solutions for low cost ONU implementation are evaluated and according to [11], there are two schemes to build this colorless ONU which should allow inexpensive production and accessible operation and maintenance processes. One scheme is to use broadband light source as the transmitter and the other is to use the ONU itself as a transmitter with injection-locked Fabry-Perot lasers combined. Moreover, [10] presents three solutions to the wavelength allocation. A solution which consists in tunable lasers that allow a desired wavelength to tune with its ONU. Another solution is use a wavelength-specific fixed tuned laser and equip each subscriber with it. And the last one, each ONU modulate the received unmodulated optical source though an external modulator or a semiconductor optical amplifier. In order to regularize the several studies concerning WDM PON technologies, a WDM PON system was standardized in ITU-T G.989 series as NG-PON2, a 40-Gigabit-capable PON as stated by [14].

2.3 Second Next Generation of Passive Optical Networks

NG-PON2 is historically the first PON system that supports multiple wavelength channels in both downstream and upstream directions. As stated by [15], NG-PON2 was originally viewed as “disruptive” with respect to the legacy optical distribution network. However the concept of NG-PON2 gradually evolved to incorporate support of the existing power-splitter-based fiber infrastructure and co-existence with the deployed legacy systems, G-PON and XG–PON. The standardized NG-PON2 ensures maximal reuse of existing technology and

compatibility with deployed optical access systems and optical fiber infrastructure.

NG-PON2 is a flexible optical fiber access network which can integrate two technologies in the same fiber infrastructure, TWDM PON and PtP WDM PON. This network is capable to provide a nominal aggregate capacity of 40 Gbps in the downstream direction and 10 Gbps in the upstream direction and to support the bandwidth requirements of mobile backhaul, business and residential services. The TWDM channels provide PtMP connectivity using conventional TDM/time division multiple access (TDMA) PON mechanisms with nominal line rates of 9.95328 Gbps and 2.48832 Gbps in both downstream and upstream directions. According to [4], TWDM PON system must support a minimum of four TWDM channels with an extension up to eight TWDM channels. The TWDM PON system is suitable for residential access.

The PtP WDM PON can be used in an overlay to TWDM with the capability of bidirectional data transmission between OLT and ONU. The PtP WDM channels provide point-to-point connectivity using some externally specified synchronous or asynchronous mechanism, such as GE or 10 GE, CPRI, or Open Base Station Architecture Initiative (OBSAI) Reference Point 3-01 (OBSAI RP3-01) specifications. The nominal line rate of PtP WDM channels is included in classes of 1.25 Gbps, 2.5 Gbps and 10 Gbps, depending on the PtP WDM client. Physical media dependent (PMD) layer requirements defines that PtP WDM must endure a minimum of four channels. The PtP WDM PON system is appropriate for business services and mobile backhauling and fronthauling services. The characteristic of a PtP WDM PON is that each ONU is served by one pair of upstream and downstream wavelengths dedicated to this ONU. On the OLT side, downstream wavelengths are multiplexed onto a shared, bidirectional fibre connecting the wavelength multiplexer (WM) to a branching node which may include any combination of power splitters, bandpass or bandstop filters, or wavelength filters.

The NG-PON2 wavelength plan is defined in [4] to enable the coexistence through wavelength overlay with legacy PON systems. The PtP WDM PON has two spectrum options for both upstream and downstream. The shared spectrum which allows full coexistence with G-PON, XG-PON1, RF video overlay and TWDM, and the expanded spectrum which supports spectral flexibility and it can be used in the absence of any one of these coexistence systems. The expanded spectrum goes from 1524 nm to 1625 nm, and the shared spectrum

is in the range 1603 − 1625 nm. On the other hand, the TWDM PON has different spectrum for each direction, for the downstream the range is 1596 − 1603 nm and for the upstream the spectrum is divided in three options: the Wideband option with 1524 − 1544 nm, the Reduced band option with 1528 − 1540 nm and the Narrow band option with 1532 − 1540 nm. All of this spectrum allows the coexistence with the previous standards as shown in figure 2.2.

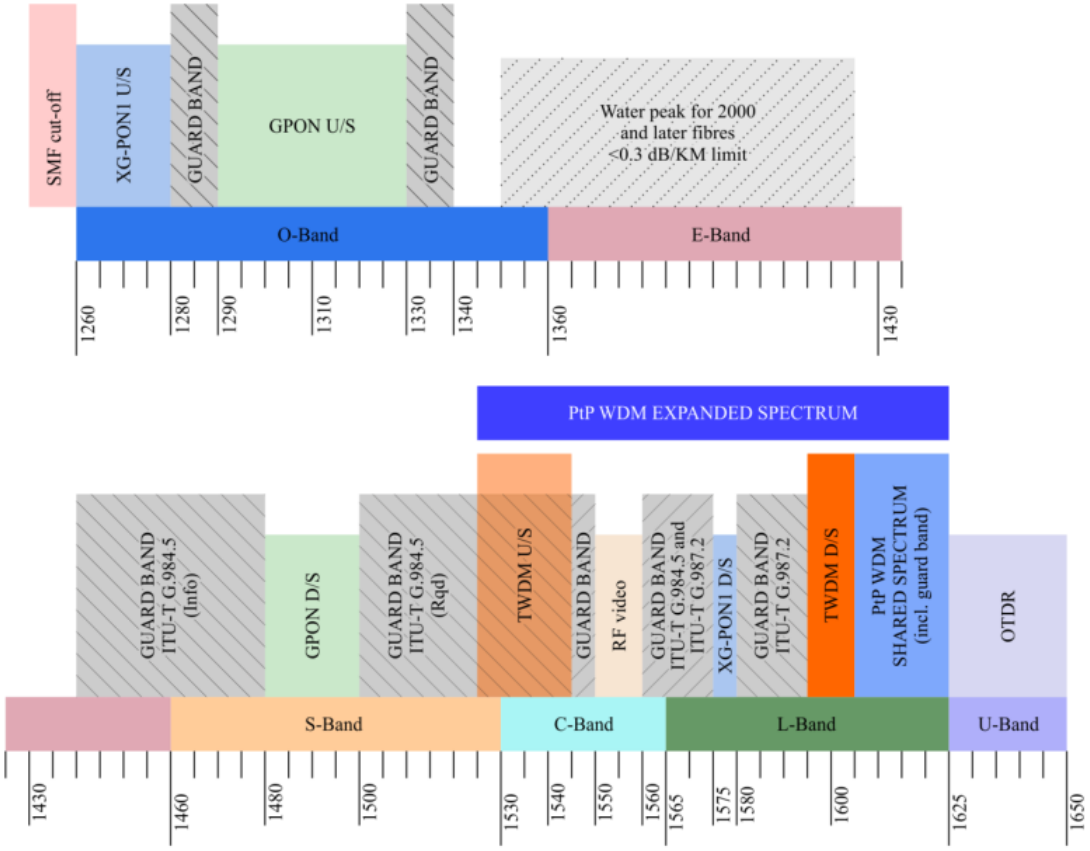

Figure 2.2: Coexistence representation of NG-PON2 Wavelength plan. Source: Appendix I from [4]

According to [4], a key feature of NG-PON2 is the ability to tune the ONU transmitter and receiver, i.e, the ability to control a tunable transceiver of an ONU to attach to any of the available TWDM or PtP WDM channels, known as wavelength channel mobility. Each TWDM channel or PtP WDM channel is associated with a single OLT channel termination (OLT CT). The OLT CTs forming a single NG-PON2 system are connected to a common trunk fiber via a WM. Whereas an active ONU has access to downstream wavelength channels, each ONU is tuned to a particular downstream wavelength channel and is transmitting at the corresponding upstream wavelength channel. A out-of-band control channel was implemented to allow the wavelength tunability and the transport of monitoring data. This channel which transmit wavelength assignment and allocation

information as well as Operation Administration and Management (OAM) data in WDM PON systems is denominated as AMCC.

2.4 Auxiliary Management and Control Channel

AMCC is a low-rate channel that allows the OLT CT and an ONU to exchange information without allocating a separate wavelength carrier while avoiding interference with inband data communication. According to [4], AMCC provides an option in a TWDM PON system to accommodate an ONU which has not been calibrated with respect to the upstream wavelength channels. However, this context represents a non-essential use case and the use of AMCC can be avoided. In the context of PtP WDM channels, AMCC can be employed to support exchange of the configuration and management information related to the multi-wavelength PON infrastructure. This usage is essential as no other means to implement the control and management (C&M) plane communications on the PON level is available.

In the PtP WDM PON, AMCC is added to each individual wavelength in both, downstream and upstream direction, according to the physical-layer implementations which determine the way the AMCC content is transported over the physical channel. This implementation consist of two alternative modes of AMCC transportation for PtP WDM channels, the transcoded mode and the transparent mode, in which the AMCC content is not affected by the mode of transport. The transcoded mode makes use of the redundancy in the underlying PtP WDM channel line codes to multiplex the PtP user data traffic and the AMCC transmission convergence (TC) traffic onto the same bit stream without changing the nominal line rate. In other words, the PtP WDN PON system converts the payload data encoding from one to another, which means that the AMCC data can be transmitted by means of code transformation. While, in the transparent mode, the AMCC TC traffic and the PtP user data traffic are handled in parallel, each provided with its own PMD interface such as optical power parameters, line codes, and modulation schemes. That is, the signals are processed individually and only at the moment of transportation the signals are summed.

The AMCC Specification is presented in Annex B from [16], relative to the transparent AMCC schemes which includes the baseband overmodulation and the RF PT schemes.

The transparent AMCC is the case where the PtP WDM PON system must transparently transport a payload bitstream, without terminating any part of its frame structure, and the AMCC has to be added to the payload at the same wavelength with only minor interference of the AMCC and the payload data. Table 2.2 resumes the characteristics of the standardized transparent AMCC scheme.

Scheme	**Baseband overmodulation**	**RF PT**
Interface	Optical	Electrical
Nominal line rate	115 kbps	128 kbps
Modulation index	10%	10%
Pulse shape	Rectangular	———
Carrier frequency	———	500 kHz

Table 2.2: Transparent AMCC schemes

Chapter 3

Mobile Network

Chapter 3 presents the Mobile Network with an overview of the network described in section 3.1 and a corresponding network evolution presented in section 3.2. Finally, the mobile network architecture is presented in section 3.3 with emphasis in the Centralized Radio Access Network.

3.1 Mobile network overview

The mobile network is also called a cellular network because it is based on the concept of cells, circular zones that overlap to cover a geographical area. Each cell provides mobile service to a limited area through its base station (BS). The BS is a radio transceiver (transmitter/receiver) located in a fixed tower, which allows communications between the mobile devices and the network, the public switched telephone network and Internet, and consequently the transmission of voice and data. This enables many mobile devices (e.g., mobile phones, tablets and laptops equipped with mobile broadband modems, pagers, etc.) to communicate with each other and with fixed transceivers and telephones anywhere in the network even if some of these mobile devices are moving through more than one cell during transmission.

The key characteristic of a cellular network is the ability to re-use frequencies to increase both coverage and capacity. A cell typically uses a distinct set of frequencies from neighbouring cells, to avoid interference and provide guaranteed service quality within each cell. There is no problem with two cells sufficiently far apart operating on the same frequency. Cell signal encoding as TDMA, frequency division multiple access (FDMA), code division multiple access (CDMA), and orthogonal frequency division multiple access (OFDMA) are

used to distinguish signals from several different transmitters.

3.2 Mobile Network Evolution

The first generation (1G) of mobile technology allowed mobile devices to connect wirelessly to the public telephone network. The 1G network was based on circuit switching and provided analog transmission of radio signals from voice traffic. Over the past decades, newer technologies have been developed and introduced in various mobile standards, thus giving rise to new generations from second generation (2G) to third generation (3G) and to the present 4G. The standards for mobile communication have been developed by consortia of network providers and operators, separately in North America, Europe, and other regions of the world.

The 2G digital mobile communications systems were introduced in 1990s to replace the 1G analog cellular networks. The first 2G standard, in Europe, was the Global System for Mobile Communications (GSM) standards, and it was developed by European Telecommunications Standards Institute (ETSI). GSM is based on the TDMA technology and provides data rates for voice services up to 13 kbps and for data services up to 9.6 kbps. The GSM standard evolved into the Generalized Packet Radio Service (GPRS) standard. GSM introduced the split-core wireless networks, in which the data transmission is made by packet-based switching technology and voice transmission by circuit-switched technology. The peak data rate of GSM is 171.2 kbps. A higher-rate modulation scheme (8-Phase Shift Keying) was introduced in Enhanced Data Rates for Global Evolution (EDGE) standard, which is the evolution of GPRS technology. With EDGE the peak data rate was further enhanced to 384 kbps.

The 3G brought the Internet for cellular subscribers. With the packet-based data, 3G was capable to support Internet applications such as email, Web browsing, text messaging, and other client-server services. The 3G standards were developed by the Third-Generation Partnership Project (3GPP), which is a global standardization organization that originally just managed the European mobile standard. The first 3G standard was the result of transition from a 2G TDMA-based GSM technology to a 3G wide-band CDMA (W-CDMA) based technology, called Universal Mobile Telecommunications System (UMTS). UMTS

was standardized in 2001 and was entitled Release 4[1] of the 3GPP standards. The downlink (DL) peak data rate of UMTS system is 1.92 Mbps. In 2002, an upgrade to the UMTS system was standardized as Release 5[2] of the 3GPP, the High-Speed Downlink Packet Access (HSDPA). The HSDPA allow faster scheduling with shorter subframes and uses a 16 Quadrature Amplitude Modulation modulation scheme, because of that the peak data rates of HSDPA is 14.4 Mbps. In 2004, the UMTS-based standard High-Speed Uplink Packet Access (HSUPA) was standardized as Release 6[3], with a maximum rate of 5.76 Mbps. The joining of HSDPA and HSUPA compound the High-Speed Packet Access (HSPA). The HSPA was upgraded and standardized as Release 7[4] of the 3GPP standard and designate as HSPA+ or Multiple Input Multiple Output (MIMO) HSDPA. The HSPA+ system can achieve a DL peak data rate of 84 Mbps.

In parallel, IEEE was developing international standards for wireless local area networks (WLANs) and wireless metropolitan area networks (WMANs). As a result, IEEE established an air-interface technology defined as OFDM in the WiFi standards 802.11a/b/g/n[5] and Worldwide Interoperability for Microwave Access (WiMAX) standards 802.16d/e[6]. The OFDM allows the system to use a certain frequency band to transmit OFDM signals with high data rates. The WiMAX standard 802.16e is known as Mobile WiMAX, provides a data rate of 26 Mbps, and it was the base for the 4G WiMAX standard.

The 4G standards features all-IP packet-based networks and supports high bandwidth applications such as mobile video-on-demand services. In 2006, IEEE standardized the IEEE 802.16m standard, also designated as WiMAX Advanced, which introduced a packet-based wireless broadband system and provides a peak date rate of 303 Mbps. Among the features of WiMAX are scalable bandwidths up to 20 MHz, higher peak data rates, and better special efficiency profiles than were being offered by the UMTS and HSPA systems at the time. An evolution of these 3GPP standards, UMTS and HSPA, is the Long Term Evolution (LTE)

[1] `http://www.3gpp.org/specifications/releases/76-release-4`
Last visited in February 14th, 2018

[2] `http://www.3gpp.org/specifications/releases/75-release-5`
Last visited in February 14th, 2018

[3] `http://www.3gpp.org/specifications/releases/74-release-6`
Last visited in February 14th, 2018

[4] `http://www.3gpp.org/specifications/releases/73-release-7`
Last visited in February 14th, 2018

[5] `https://standards.ieee.org/develop/wg/WG802.11.html`
Last visited in February 14th, 2018

[6] `http://standards.ieee.org/develop/wg/WG802.16.html`
Last visited in February 14th, 2018

standard designated as 3GPP release 8 standard[7]. In addition to inheriting from previous 3GPP standards, LTE features the OFDM from the 802.16e standard, and provides a maximum data rate of 300 Mbps. The LTE-Advanced is an evolution of LTE which was added technologies as carrier aggregation, enhanced DL MIMO, uplink (UL) MIMO, and relays. Which improved the spectral efficiency, peak data rates, and user experience. The LTE-Advanced was standardized as 3GPP version 10[8], with a maximum peak data rate of 1 Gbps.

The table 3.1 resumes the information about the mobile standards presented in this section. Relative to the maximum data rates offered by these standards, the progress in peak data rates is visible. The maximum data rates of LTE and LTE-Advanced standards are about 2000 times above what was offered by GSM/EDGE technology and 50–500 times above what was offered by the W-CDMA/UMTS systems.

3.2.1 Long Term Evolution

LTE requirements cover two fundamental components of the evolved UMTS system architecture: the Evolved Universal Terrestrial Radio Access Network and the Evolved Packet Core. LTE specifies data communications protocols for both the UL, mobile to base station, and DL, base station to mobile communications. In the DL case, the LTE air interface is based on OFDM multiple-access technology. Which provides high spectral efficiency and adaptability for broadband data transmission, resistance to intersymbol interference caused by multipath fading, a natural support for MIMO schemes, and support for frequency-domain techniques such as frequency-selective scheduling [17]. However, OFDM multicarrier transmission causes large variations in the instantaneous transmit power, which implies a reduced efficiency in power amplifiers and results in higher mobile-terminal power consumption. For that reason, the LTE air interface in the UL is based on Single-Carrier Frequency Division Multiplexing which substantially reduces fluctuations of the transmited power. The resulting UL transmission scheme can still feature most of the benefits associated with OFDM, such as low-complexity frequency-domain equalization and frequency-domain scheduling, with less stringent requirements on the power amplifier design. The time-frequency representation of OFDM is designed to provide high levels of

[7] `http://www.3gpp.org/specifications/releases/72-release-8`
Last visited in February 14th, 2018

[8] `http://www.3gpp.org/specifications/releases/70-release-10`
Last visited in February 14th, 2018

Year	Generation	Standard	Technology	Peak data rate	standardization organization
1990	2G	GSM	TDMA	9.6 kbps	ETSI
2000		GPRS		171.2 kbps	
2001	3G	UMTS (Release 4)	W-CDMA	1.92 Mbps	3GPP
2002		HSDPA (Release 5)	W-CDMA	14.4 Mbps	
2003		EDGE	TDMA	384 kbps 473 kbps	ETSI
2004		HSUPA (Release 6)	W-CDMA	5.76 Mbps	3GPP
2005		Mobile WiMAX (802.16e)	OFDMA	26 Mbps	IEEE
2006		HSPA+ (Release 7)	W-CDMA	84 Mbps	3GPP
2008	4G	LTE (Release 8)	OFDMA	300 Mbps	
2011		WiMAX advanced (802.16m)		303 Mbps	IEEE
2011		LTE Advanced (Release 10)	OFDMA	1 Gbps	3GPP

Table 3.1: Mobile standards

flexibility in allocating both spectra and the time frames for transmission. The spectrum flexibility in LTE provides not only a variety of frequency bands but also a scalable set of bandwidths.

The LTE standards specify the available radio spectra in different frequency bands which includes the frequency bands defined for previous 3GPP standards, thus allowing seamless integration with previous mobile systems. The regulations governing these frequency bands vary between different countries. Therefore, it is conceivable that not just one but many of the frequency bands could be deployed by any given service provider to make the global roaming mechanism much easier to manage. LTE supports frequency division duplex (FDD) mode, in which frequency bands are specified as paired spectra, and time division duplex (TDD) mode with frequency bands specified as unpaired spectra. The paired FDD frequency bands enables simultaneous transmission on two frequencies: one for the DL and one for the UL. For improved receiver performance, the paired bands are specified with sufficient separation. The unpaired TDD frequency bands share the same channel

and carrier frequency by the UL and DL transmissions, which are time-multiplexed. The comprehensive list of ITU International Mobile Telecommunication (IMT), IMT-Advanced[9], frequency bands is presented in Release 11 of the 3GPP specifications for LTE. It includes 25 frequency bands for FDD, where each paired band are indexed from 1 to 25, and 11 frequency bands for TDD, where the unpaired bands are numbered from 33 to 43. For example, band number 1 corresponds to the paired bands used in FDD duplex mode with a UL operating band frequency range in $1920 - 1980$ MHz, and DL in $2110 - 2170$ MHz. However, the operating band index 6 is not applicable to LTE and bands 15 and 16 are dedicated to ITU Region 1. The IMT-Advanced indicates a list of spectrum allocations ranging from 1.4 to 20 MHz which enables scalability in the frequency domain, and consequently leads to spectrum flexibility.

The frequency spectra in LTE are formed as concatenations of resource blocks. A resource block consist in 12 adjacent subcarriers grouped together and has a total bandwidth of 180 kHz, since 15 kHz separates subcarriers. This 180 kHz is the smallest bandwidth unit assigned by the BS scheduler, and enables transmission bandwidth configurations of from 6 to 110 resource blocks over a single frequency carrier, which explains how the multicarrier transmission nature of the LTE standard allows for channel bandwidths ranging from 1.4 to 20.0 MHz in steps of 180 kHz, allowing spectrum flexibility. To minimize latency, LTE specifies a short frame size of 10 ms, which allows timely feedbacks necessary for link adaptations to be provided to the base station.

3.3 Mobile Network Architecture

In 1G and 2G mobile networks, radio and baseband processing functionalities are integrated inside a BS. The radio equipment at these conventional cell sites is located at the base of the tower, transmitting RF signals via coax to antennas at the top of the tower. However, these coax-based feeders produce most problems in cell sites due to their inherent loss and susceptibility to interference. In addition, environmental conditions deteriorate cables and connectors, creating signal reflections and intermodulation.

In 3G and 4G cellular networks, the radio equipment is divided into two main elements:

[9] `https://www.itu.int/en/ITU-R/study-groups/rsg5/rwp5d/imt-adv/Pages/default.aspx` Last visited in February 14th, 2018

a radio unit (RU) and a digital unit (DU), giving rise to a distributed RAN. The RU performs RF functions on an analog domain, and it is installed next to the antennas at the top of the tower. The DU performs radio functions on a digital baseband domain, and resides at the base of the tower or at a few meters of distance allowing a low site rental and convenience of maintenance. These two radio elements, the DU and RU, are connect by a coax or fiber cable. In the 4G beyond, the DUs corresponding to several cell sites were moved to a common central location serving a large group of RUs, which are connected via fiber links. This new architecture is known as C-RAN. The evolution of mobile network architecture is shown in figure 3.1.

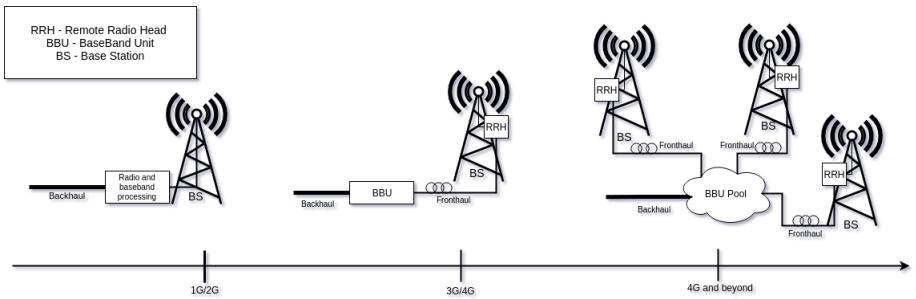

Figure 3.1: The evolution of BS.
Figure adapted from [5]

3.3.1 Centralized Radio Access Network

In C-RAN architecture, the RU could be called radio equipment (RE), remote radio head (RRH), or remote radio unit, and the DU could be called radio equipment control (REC), or baseband unit (BBU). The C-RAN concept has been recognized as an evolved system paradigm that offers cost savings by allowing for relaxed hardware specifications (environmental hardening is needed for only a few components), by requiring a smaller footprint and less power consumption of outdoor equipment, by sharing infrastructure in the BBU location, by simplifying repair and maintenance, and by easing system upgrades. In addition to these capital expenditure and operational expenditure benefits, the C-RAN architecture also eases the implementation of advanced radio transmission techniques that have been considered for helping improve RAN coverage, bit rate, and throughput by way of intercell cooperation such as the coordinated multipoint operation. A representation of C-RAN architecture is shown in figure 3.2. It is important to note that Centralized-RAN is not the same as Cloud-RAN, since Cloud-RAN is an enhanced Centralized-RAN with virtualization.

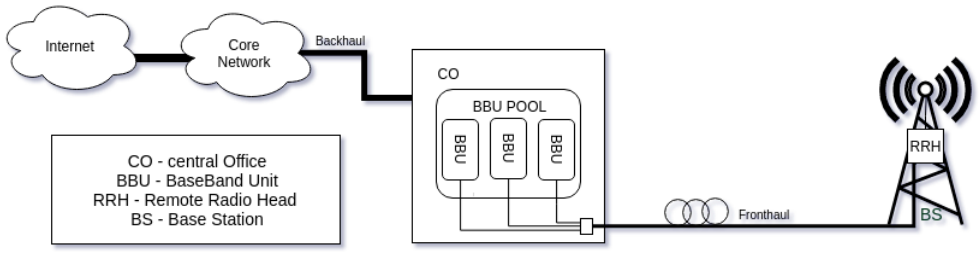

Figure 3.2: Centralized RAN

Regarding the cooperation between BBUs and RRHs and regarding the implementation of the BBU functionalities, the C-RAN architecture can be implemented in BBU hotel, BBU pool, and BBU cloud. In BBU hotel variation, many BBUs are collocated, but remain separate and are each individually connected to a dedicated RRH. Whereas in BBU pool, a cluster of collocated and cooperating BBUs serves a cluster of RRHs. In the BBU cloud, the processing functions of a BBU pool are implemented on servers that can be flexibly configured, and the processing load can be shifted between different pools in different locations.

In addition to BBU and RRH, C-RAN is composed of two more elements, the backhaul and fronthaul. The backhaul is the responsible for the connection between the BBU and the core network, and backhaul links extend over long distances of up to several tens or even hundreds of kilometres. Whereas the fronthaul is the segment which connects the RRH and BBU. Fonthaul uses a D-RoF interface to manage the link between the REC and the RE, and the functions of each one. The D-RoF interface is specified in CPRI[10], OBSAI[11] specifications, and Open Radio Interface (ORI)[12].

CPRI initiative aims at defining a publicly available specification of the protocol interface between DU and RU. The first version of CPRI specification was released at the end of 2003. It deals with the physical layer and with layer 2, defining a frame that contains I and Q samples resulting of radio signal digitization, synchronization information and some C&M information. The physical layer is typically optical fiber based on small form

[10] `http://www.cpri.info/`
Last visited in February 14th, 2018
[11] `http://www.obsai.com/specifications.htm`
Last visited in February 14th, 2018
[12] `http://www.etsi.org/technologies-clusters/technologies/ori`
Last visited in February 14th, 2018

factor pluggable (SFP) connectivity. CPRI is an industry standard aimed at defining a publicly available specification for the internal interface of wireless base stations between the BBU and RRH, that is, CPRI specification describes the interface connecting BBU and RRH.

The OBSAI is another industry initiative joining BS vendors, module and component manufacturers. OBSAI aims at creating an open market for cellular BSs and hence substantially reducing the development effort and costs associated with creating new BS product ranges. OBSAI specifications cover the areas of Transport, Clock/Control, Radio and Base Band, as well as interfaces and conformance test specifications. OBSAI was first established in 2002 and successive versions have been released in the last years. A similar specification was developed by OBSAI which defines a set of specifications providing the architecture, function descriptions, and minimum requirements for integrating common modules into a base transceiver station. More specifically, reference point 3 (RP3) interchanges user and signaling data between the BBU and the RRH. The main network-element manufacturer members of OBSAI include ZTE, NEC, Nokia Siemens Networks, Samsung, and Alcatel Lucent.

The ORI is an Industry Specification Group (ISG) initiated in May 2010 by ETSI. ORI goal is to develop an interface specification envisioning interoperability between elements of BSs of cellular mobile network equipment. ORI eliminates proprietary implementations and achieves interoperability between multi-vendor BBUs and RRHs. The interface defined by the ORI ISG is built on top of the CPRI with the removal of some options and the addition of other functions so to reach the full interoperability. ORI specifications are based on CPRI and expand on the specifications of the interface.

As [18] indicates: a main difference between CPRI, OBSAI, and ORI is the fact that the first two groups are composed only by equipment makers, whereas ORI members include also several network operators. Despite a few differences between CPRI, OBSAI and ORI, some key common aspects are the following: All BSs are split in two parts connected with fronthaul interface, the fronthaul most adapted physical layer is optical fiber, fronthaul interface is implemented in SFPs that constitute the “de facto” connectivity in all RUs and DUs, and Fronthaul interface presents a constant bit rate (CBR) in UL and DL. According to [18], CPRI is currently the most adopted specification for fronthaul interface implementation.

Chapter 4

Common Public Radio Interface

Chapter 4 introduces and defines the CPRI interface. The specification of the interface is described in section 4.1 and the converted process from radio signal to CPRI signal is presented in section 4.2. Finally, a contextualization of CPRI in C-RAN based LTE scenarios is presented in section 4.3.

4.1 Interface Specification

After the first version of CPRI specification was released, further versions have been published until version seven in 2015. CPRI is a CBR radio interface whose specification has been developed by Ericsson AB, Huawei Technologies Co. Ltd, NEC Corporation, Alcatel Lucent and Nokia Networks. However, CPRI is an industry agreement with the option to include proprietary information that limits the terrestrial RAN sharing, the RAN reconfigurability, and thus capital expenditure and operational expenditure savings. It must be noted that CPRI is not a standard, but an industry agreement. It still contains vendor specific elements and hence does not guarantee full interoperability. It does not contain specifications of an optical transport layer, but merely recommends using existing optical hardware such as that used for high-speed serial links for Ethernet, or Fiber Channel transmission. CPRI supports a wide variety of radio standards: Universal Terrestrial Radio Access (UTRA) FDD, WiMAX, Evolved UTRA (E-UTRA, LTE), and GSM/EDGE.

4.1.1 Protocol Overview

As indicated in [6], the CPRI protocol is defined in Layer 1, and Layer 2. The Layer 1 covers all the physical transmission aspects between the BBU and RRH including electrical

and optical media and their corresponding line rates. While, the Layer 2 defines the main data flows, which are user plane (U-plane) data, C&M data, and synchronization data.

The U-plane data are U-plane information transported in the form of digital baseband signals, in-phase and quadrature (IQ) data flows. Each IQ data flow reflects the radio signal, sampled and digitalized, of one antenna carrier (AxC). An AxC is a carrier at one independent antenna element. The IQ data of different AxCs are multiplexed by a time division multiplexing scheme onto an electrical or optical transmission line. In this work the transmission line in use is the optical one.

The C&M data are exchanged between the C&M entities within the BBU and the RRH. This information flow is given to the higher protocol layers, and can be transmitted by either an in-band protocol used for time-critical signaling data, or by layer 3 protocols, which is not defined by CPRI, that reside on top of appropriate layer 2 protocols. The inband protocol is a signaling information used for synchronization and timing, which is directly transported by the physical layer and is related to the link layer. It is used also for error detection and correction with the implementation of the line codes 8B/10B and 64B/66B, specified in IEEE 802.3, the line code violations allow link failures and synchronization issues to be detected by the physical layer. CPRI supports two different layers 2 protocols for C&M data: the subset of High Level Data Link Control (HDLC) and Ethernet. The additional C&M data are time multiplexed with the IQ data onto a digital serial communication line.

The synchronization data is used for frame and time alignment. There is the Vendor Specific Information which is the information flow reserved for the transfer of any type of vendor specific information in additional time slots. Figure 4.1 provides an overview on the basic protocol hierarchy.

4.1.2 Physical Layer Specifications

The physical layer specifications from [6] includes topics such as Physical Layer Modes, Electrical Interface, Optical Interface, Line Coding, Bit Error Correction/Detection, Synchronization and Timing, Link Delay Accuracy and Cable Delay Calibration, and Link

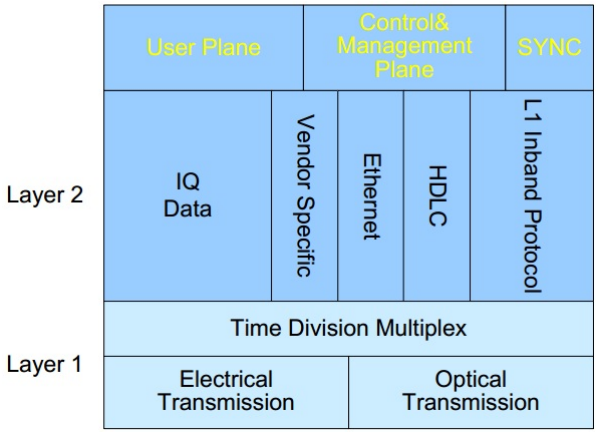

Figure 4.1: CPRI protocol overview. Source: [6]

Maintenance of Physical Layer, Line Bit Rate, and Frame Structure. This subsection focuses on these last two topics.

Line bit Rate

CPRI is a CBR interface with line bit rates options that go from 614.4 Mbps (option 1) up to 24.33 Gbps (option 10) based on UMTS to provide the flexibility to accommodate different signal bandwidths. All CPRI line bit rates have been chosen in such a way that the UMTS basic chip rate of 3.84 Mbps can be recovered in a cost-efficient way from the line bit rate considering the line coding scheme. For example, the 1.2288 Gbps correspond to an encoder rate of 122.88 MHz for the 8B/10B encoder and a subsequent frequency division by a factor of 32 provides the basic UMTS chip rate.

Options	Rate (Gbps)	Line coding
1	0.6144	8B/10B line coding (1 x 491.52 x 10/8 Mbps)
2	1.2288	8B/10B line coding (2 x 491.52 x 10/8 Mbps)
3	2.4576	8B/10B line coding (4 x 491.52 x 10/8 Mbps)
4	3.0720	8B/10B line coding (5 x 491.52 x 10/8 Mbps)
5	4.9152	8B/10B line coding (8 x 491.52 x 10/8 Mbps)
6	6.1440	8B/10B line coding (10 x 491.52 x 10/8 Mbps)
7	9.8304	8B/10B line coding (16 x 491.52 x 10/8 Mbps)
7A	8.11008	64B/66B line coding (16 x 491.52 x 66/64 Mbps)
8	10.1376	64B/66B line coding (20 x 491.52 x 66/64 Mbps)
9	12.16512	64B/66B line coding (24 x 491.52 x 66/64 Mbps)
10	24.33024	64B/66B line coding (48 x 491.52 x 66/64 Mbps)

Table 4.1: CPRI line bit rate

As indicated in [6] the line bit rate option 7A whose bit rate is 8.11008 Gbps is diferrent

from option 7 for having a different line coding scheme and a lower line bit rate so it can be used for intra-REC and/or intra-RE electrical interface only, which is the purpose.

Frame structure

CPRI defines a hierarchical framing with three layers: the basic frame, the hyperframe, and the CPRI frame. A basic frame is created and transmitted every T_c defined by equation (4.1), which is based on UMTS clock rate, that is, 3.84 MHz. This duration remains constant for all CPRI line bit rate options.

$$T_c = \frac{1}{f_c} = \frac{1}{3.84MHz} = 260.416667\text{ns} \tag{4.1}$$

Each basic frame consists of W = 16 words (W = 0, ..., 15), and the length T of each word depends on the CPRI line bit rate option. Consequently, the size of a basic frame is variable as we can see in table 4.2. The first word W = 0 is the control word (CW). It is reserved for control and carries C&M information. The remaining words (W=1...15), 15/16 of the basic frame, are dedicated to the U-plane IQ data transport (IQ data block).

Options	1	2	3	4	5	6	7	7A	8	9	10
T [bytes]	1	2	4	5	8	10	16	16	20	24	48

Table 4.2: length T of CPRI word

A hyper frame is made of 256 basic frames, and it is created every $256 \times T_c = 66,67\mu s$. Each hyperframe has 256 CWs and these 256 CWs are organized into 64 subchannels of 4 CWs each. Every CW can be addressed by a subchannel ID (0, ..., 63). Each subchannel belongs to one category out of seven: Synchronization, L1 In-Band Protocol, Slow C&M Link, $Ctrl_{AxC}$, Fast C&M Link, and Reserved for Future Use and Vendor-Specific.

A collection of 150 hyperframes make a CPRI frame, and it is created every $150 \times 66,67$ $\mu s = 10ms$. The CPRI line rate information is sent in a Z.Y.W.X format, where Z is the hyper frame number, Y is the basic frame within a hyper frame, W is the word number within a basic frame, and X is the byte number within a word. The CPRI frame hierarchy

is represented in figure 4.2.

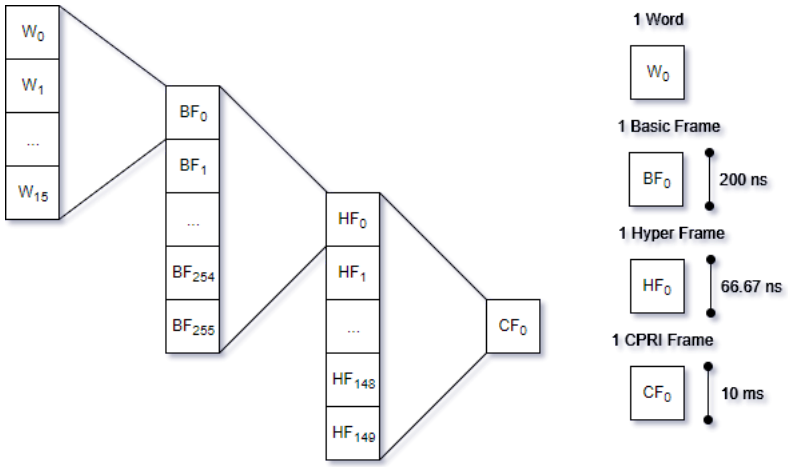

Figure 4.2: CPRI frame hierarchy

4.2 Radio signal to CPRI signal

According to [19], the creation of a CPRI signal from an analog signal is made in four steps: sampling, mapping, grouping, and framing. The first stage is the sampling, where the radio signal is sampled and then quantized. The transmission of data is based on the concept of an AxC. One AxC is the amount of digital baseband (IQ) data necessary for either reception or transmission of only one carrier at one independent antenna element. The amount of information carried by an AxC depends on the sampling frequency fs and the number of bits M used in the quantization process of the in-phase (I) and quadrature-phase (Q) radio signals. The sampling frequency is a multiple of the nominal chip rate fc = 3.84 MHz, If signals do not equate to a multiple integer, stuffing samples are added, and on the radio signals are analyzed considering both I and Q components. The I and Q components are sampled and characterized digitally based on the number of sampling bits assigned to represent this information. CPRI indicates that one IQ sample consists of one I sample and one equal-sized Q sample, with width M for DL and M' for UL. The number of sample bits M ranges from 8 to 20 bits, and M' from 4 to 20 bits. One AxC comprises M + M = 2M bits/IQ sample.

In the mapping stage, the I and Q samples are consecutively mapped in chronological order and consecutively into containers defined as AxC containers and are transported by only one carrier at one independent antenna. An AxC Container is a sub-part of the IQ data block of one basic frame. The size of an AxC Container, NAxC, is always an even

number of bits. In the standard case IQ samples shall be sent in an AxC Container in chronological order and consecutively, from Least Significant Bit (I0, Q0) to Most Significant Bit (IM-1, QM-1) or (IM'-1, QM'-1), or I and Q samples being interleaved. CPRI defines 3 mapping methods: IQ sample based, WiMAX symbol based, and backwards compatible. IQ sample based method is intended for dense packing of IQ data into the CPRI data flow (high bandwidth efficiency) and is optimized for low latency together with sample based processing of IQ data in the RRH(s). For this mapping method the size N_{AxC} of the AxC Container shall be chosen according to equation (4.2), where M is the number of sampling bits for DL case, f_s is the sampling rate, and f_c is the UMTS chip rate of $3.84MHz$. M' shall be used instead of M for the UL case. The WiMAX symbol based is the mapping method intended for dense packing of IQ data into the CPRI data flow and is optimized for low latency together with WiMAX symbol based processing of IQ data in the RRH(s). The length K of the AxC Container Block shall be chosen equal to the WiMAX frame duration T_f, as described by the given equation (4.3). K is an integer for all WiMAX frame durations T_f. The backward compatible mapping method defines the size of the AxC Container $N_{AxC} = 2 \times M$ with M being the number of sample bits. This methodology defines an AxC containing exactly one sample (or stuffing bits for LTE and GSM signals). According to [19], the IQ sample based and backwards compatible are the most applicable mapping methods in mobile networks.

$$N_{AxC} = 2 \times \left[\frac{M \times f_s}{f_c} \right] \tag{4.2}$$

$$K = T_f \times f_c \tag{4.3}$$

In the grouping stage, multiple AxC containers are grouped into a IQ data block. The following mapping rules apply for both, UL and DL: each AxC Container is sent as a block, overlap of AxC Containers is not allowed, and the position of each AxC Container in the IQ data block is decided by one of the following options: Option 1 (packed position) or Option 2 (flexible position). There are two available options to group the AxC containers: the packed position and flexible position. In packed position each AxC container is sent consecutively without any reserved bits in between, and in ascending order of AxC number. While in flexible position each AxC container is sent with an index indicating the number of reserved bits existing between each AxC container. For each AxC Container, the application

shall decide at what address (W, B – for $W > 0$) in the IQ data block the first bit of the AxC Container is positioned. The first bit of an AxC Container shall be positioned on an even bit position in the IQ data block (B shall be even).

In the last stage, the framing stage, the CPRI frame structure described in previous subsection are created. As we know the basic frame are composed by 16 words, the first word correspond to the CW and the remaining 15 words corresponds to the IQ data block formed in the mapping stage. The composition of 256 basic frames gives us the hyper-frame, and the composition of 150 hyperframes gives us the CPRI frame. Then, the CPRI frame is line coding by 8-bit to 10-bit symbol coding to balance DC power and recover synchronization. This all steps are the basis for RF over CPRI transmission, where an analog radio signal was converted into a CPRI signal, a baseband signal, and it is ready for transmission over the fronthaul. Figure 4.3 resumes the stages of the creation of a CPRI signal from a radio signal.

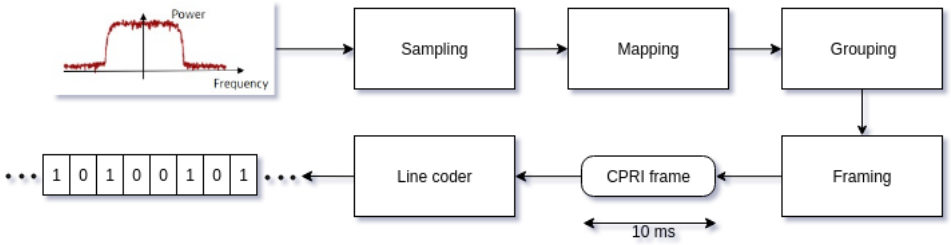

Figure 4.3: Radio signal to CPRI signal

4.3 CPRI in C-RAN based LTE Scenarios

As present in section 3.3.1 the C-RAN architecture is composed of RRH, fronthaul, BBU, and backhaul. The RRH and BBU are the components in which its functions depend on if is a radio transmission, DL, or if is a radio reception, UL. In the UL case, the transceiver in the base station receive the RF signals, and the RRH performs the sampling of the radio signal. The resulting data is sent to the BBU over the fronthaul. Figure 4.4 represents a conceptual explanation of RRH/BBU functional split in upstream direction.

The RRH provides the analogue and radio frequency functions such as filtering, modulation, frequency conversion and amplification. Whereas, the BBU is the interface with the core network via the backhaul. It is concerned with the Network Interface transport, the

radio base station C&M as well as the digital baseband processing. All the operations above the physical layer and digital baseband processing are performed by BBU, such as channel decoding, de-interleaving, demodulation, MIMO processing, transmit power control, and signal distribution for processing.

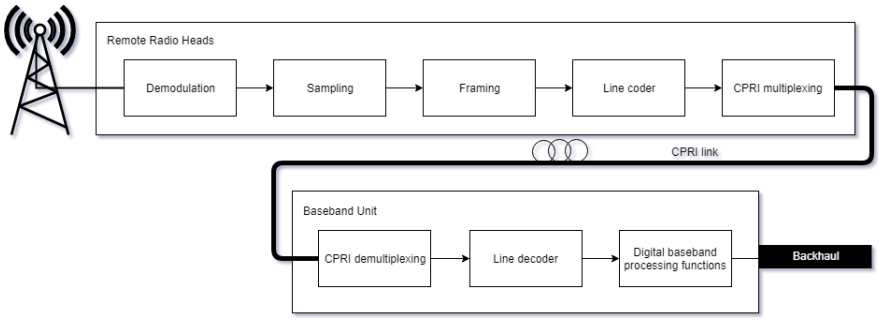

Figure 4.4: Conceptual explanation of RRH/BBU functional split in upstream direction. Figure adapted from [7]

As we see in 4.1.1, the transmission of U-plane data is based on the concept of an AxC (AxC). Given that the LTE radio signal is first sampled and then quantized so it can converted in CPRI signal. The sampling frequency, f_s, is a multiple of the nominal chip rate $f_c = 3.84$ MHz, and it is defined in equation (4.4) per 10 MHz radio bandwidth, so by the cross-multiplication we have equation (4.5).

$$f_s = \frac{15.36 M_{samples}}{s} \tag{4.4}$$

$$f_s = \frac{\frac{15.36 M_{samples}}{s} \times \text{carrier}}{10 MHz} \tag{4.5}$$

As indicated in [7] the number of bits per sample, b_s, used in the quantization process of the I and Q radio signals, for capacity efficiency for a LTE or LTE-Advanced signal should be $b_s = 15$. With this two parameters defined, a data bit rate needed for the sampling and quantization of an AxC can be obtain from the following equation (4.6).

$$B_{AxC} = f_s \times 2 \times b_s \times CW \times LC \tag{4.6}$$

Where the multiplication factor 2 considers the separate processing of I and Q samples, $CW = \frac{16}{15}$ represents the factor of CPRI CW considering the additional overhead information, and LC is the coding factor considering the rate increase caused by line coding, $LC = \frac{10}{8}$ for 8B/10B coding, and $LC = \frac{66}{64}$ for 64B/66B coding.

Table 4.3 presents the data rate per AxC for LTE channel bandwidth from 1.25 MHz to 20 MHz using the 8B/10B line coding. Whereas, table 4.4 presents the data rate per AxC for LTE channel bandwidth from 1.25 MHz to 20 MHz using the 66B/640B line coding.

LTE channel bandwidth (MHz)	1.25	2.5	5	10	15	20
Data rate per AxC, B_{AxC} (Mbps)	76.8	153.6	307.2	614.4	921.6	1228.8

Table 4.3: the bit rate required per AxC for different LTE bandwidths for 8B/10B line coding

LTE channel bandwidth (MHz)	1.25	2.5	5	10	15	20
Data rate per AxC, B_{AxC} (Mbps)	63.36	126.72	253.44	506.88	760.32	1013.76

Table 4.4: the bit rate required per AxC for different LTE bandwidths for 66B/64B line coding

The length T of a word in a basic frame depends on the CPRI data rates, which means that the number of AxC of channel bandwidth depends on the CPRI data rates. In this light, table 4.5 shows the bit rate required per AxC for different LTE bandwidths and the maximum number of AxCs transported for standard CPRI bit rates. As examples, CPRI bit rate 2.4576 Gbps can carry 32 AxCs from 1.25 MHz LTE channel, 16 AxCs from 2.5 MHz, or 1 AxC from 20 MHz. Whereas, CPRI bit rate 10.1376 Gbps can carry 160 AxCs from 1.25 MHz LTE bandwidth, 80 AxCs from 2.5 MHz, or 10 AxCs from 20 MHz. Thus, this table allows the dimensioning of fronthaul networks in C-RAN scenarios according to specific requirements. Taking into account that real implementations of remote sites frequently contain multiple antennas for a single or for multiple different mobile network operators (MNOs), for multiple Radio Access Technologies, and/or for MIMO radio configurations, and that each antenna is individually assigned its own dedicated IQ data flows, the table 4.5 can be read in another perspective. As an example, if the LTE setup is fixed to a number of 3 sectors and 2×2 MIMO with a 10 MHz LTE bandwidth (i.e., 2×3 AxCs), a lookup in table 4.5, column "10 MHz LTE bandwidth" reveals that at least CPRI bit rate 4.9152 Gbps is required to carry such a number of AxC.

Another way to know the corresponding CPRI line rates for some LTE site configurations

		Number of AxCs of channel bandwidth and bit rate required per AxC					
CPRI data rate (Gbps)	**T**	**1.25 MHz (76.8 Mbps)**	**2.5 MHz (153.6 Mbps)**	**5 MHz (921.6 Mbps)**	**10 MHz (614.4 Mbps)**	**15 MHz (921.6 Mbps)**	**20 MHz (1228.8 Mbps)**
0.6144	8	8	4	2	1	-	-
1.2288	16	16	8	4	2	1	1
2.4576	32	32	16	8	4	2	1
3.072	40	40	20	10	5	3	2
4.9152	64	64	32	16	8	5	4
6.144	80	80	40	20	10	6	5
9.830.4	128	128	64	32	16	10	8
		(63.36 Mbps)	**(126.72 Mbps)**	**(253.44 Mbps)**	**(506.88 Mbps)**	**(760.32 Mbps)**	**(1013.76 Mbps)**
8.11008	128	128	64	32	16	10	8
10.1376	160	160	80	40	20	13	10
12.16512	192	192	96	48	24	16	12

Table 4.5: Maximum number of AxC transported in a CPRI link, $M = 15$ bits, adapted from [7]

is to calculate the total bit rate for the CPRI fronthaul links using the equation for multi-sector and multi-antenna configurations given by equation (4.7), where S is the number of sectors, A is the number of antennas per sector.

$$B_{CPRI} = S \times A \times f_s \times 2 \times b_s \times Cw \times LC \tag{4.7}$$

Examples from [20] indicates that a macro cell for 2 MNOs each with 3 sectors and 2×2 MIMO, (20 + 20) MHz requires a CPRI bit rate of 29.5 Gbps. While a tower with 3x(4x4 MIMO)x(20+20) MHz, 3x(2x2 MIMO)x20 MHz, and 1x(8x8 MIMO)x(20+20) MHz requires a CPRI bit rate of 56.6 Gbps. Another few examples are presented in table 4.6.

S		A	**Carrier (MHz)**	f_s **(Msample/s)**	LC	B_{CPRI} **(Gbps)**
1	2x2 MIMO	2	20	30.72	10/8	2.4576
1	4x4 MIMO	4	20	30.72	10/8	4.9152
3	2x2 MIMO	2	40	61.44	10/8	14.746
3	8x8 MIMO	8	100	153.6	10/8	147.456

Table 4.6: CPRI line rates for some LTE site configurations

The main requirements for CPRI transmission apart from the required bandwidth are delay and bit error rate (BER). CPRI links should operate with at most 5 ms delay contribution excluding propagation delay, and a maximum allowed BER of 10^{-12}. In addition, the

frequency deviation from the CPRI link to the radio BS must be not larger than 0.002 parts per million. Forward error correction (FEC) is not precluded, but neither is it recommended.

Regarding on constraints in fronthaul transport imposed by LTE, the typical latency for the fronthaul transport segment for carrying antenna data is of the order of a few hundred microseconds and it depends on the UL hybrid automatic repeat request process, in which the BBU must indicate within 4 ms to the user equipment to retransmit an erroneous packet. This transmission latency relates to the round-trip time from the RRH to the BBU and the return, including the travel time over the fiber as well as the signal processing time in the optical system equipment. Depending on the optical transmission technology, the fiber length between BBU and RRH is thus typically limited to below 20 km. CPRI equipment must support an operating range of at least 10 km.

Chapter 5

Mobile fronthaul supported by PtP WDM-PON

This chapter presents the state of the art research on some relevant topics on convergence of NGMN with particular emphasis on mobile fronthaul (MFH) supported by PtP WDM-PON enabled by the AMCC signaling channel.

5.1 Basic architecture

NG-PON2 based on WDM is considered a promising access network architecture allowing wavelength tunability [21]. The wavelength tunability at the ONU provides dynamic wavelength allocation functions. Wavelength tunability is also important in the context of 5G networks supported by NG-PON2 PtP WDM PON to achieve fronthaul transport. In a WDM-PON the ONU should be wavelength agnostic, i.e, it should be able to operate at several wavelengths. WDM PON has been proposed by G989.1 with some restrictions under the name PtP WDM PON to among other applications carry wireless services. In the fronthaul context, a wavelength or more should be allocated for the support of a given RRH. The wavelength allocation is not fixed, it is provided dynamically depending on the network needs. As shown in figure 5.1. In systems of this type, the AMCC provides network management functions, (e.g., wavelength allocation, wavelength calibration).

5.2 AMCC implementation

Two implementation methods are referred in the literature: the in-of-band and the out-of-band methods. In the in-of-band method the AMCC information is embedded on the

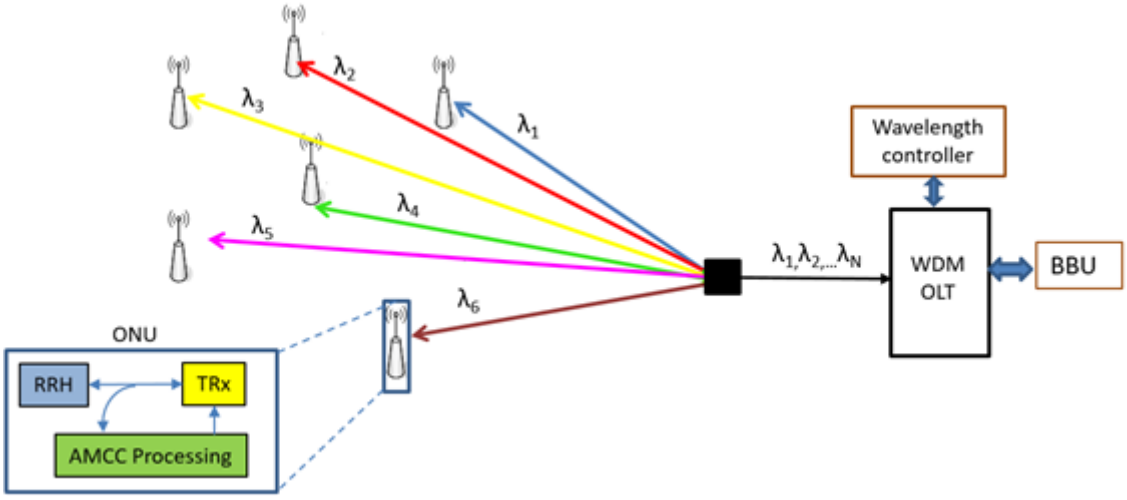

Figure 5.1: Illustrative architecture of a WDM-PON with AMCC for MFH support.

CPRI signal and is transported using vendor reserved bits. This approach does not require additional circuits or filtering. The main disadvantage is the limited capacity reserved in each CPRI frame structure.

In out-of-band methods the management and control information is transported through a different transmission channel. This method enables a management and control channel to be established independently from the frame structure of the client signal. However, it requires additional circuits.

5.3 AMCC implementation using out-of-band methods

Since AMCC channel was introduced in NG-PON2 standard, different out-of-band implementation approaches have been proposed. AMCC reported implementations follow basically three approaches: a) superimposition on main data signal, which can be done by baseband intensity over-modulation scheme [22], b) by RF tone modulation [23] and [24], and c) by a cascaded phase overmodulation scheme [8].

In this dissertation we will focus on AMCC implementation using digital modulation of an RF carrier. At the OLT side, the PT is modulated by the management information (e.g., wavelength allocation, wavelength calibration) and superimposed electrically to the client signal by using a low-frequency carrier wave such that it does not impair the transmission of the CPRI signal. At the ONU side, the embedded PT is demultiplexed after the optical signal

is detected and an AMCC processing unit is used to extract the wavelength management information.

5.4 AMCC implementation using RF carrier tone

In [23], it is proposed a WDM-PON system architecture with an AMCC to support MFH. The AMCC was transmitted using a PT. At the OLT side, the PT is modulated by the management information and superimposed electrically to the CPRI signal by using a low-frequency carrier wave. At the ONU side, serving a RRH, the embedded PT is demultiplexed after the optical signal is detected and an AMCC processing unit is used to extract the management information. The AMCC channel is inserted in each wavelength for the upstream and downstream.

The optical transmitter consisted of a DFB laser followed by a Mach-Zehnder Modulator (MZM) driven by the multiplexed AMCC and CPRI. Two CPRI options corresponding to 2.4576 Gbps (option 3) and 9.8304 Gbps (option 7) were tested. It was confirmed that it was feasible to insert a PT of 500 kHz with a 128 kbps line rate and -20 dB modulation index. The modulation index was defined as the ratio of the voltage amplitude between the PT and the main signal in the electrical domain. The performance of this scheme relies on the modulation depth of AMCC message signal. An increase in the modulation depth of AMCC message decreases the performance of CPRI data.

AMCC implementation by PT implementation was also implemented in systems using a Directly Modulated Laser of a commercial SFP over a 20 km fronthaul link [9]. A 128 kbps AMCC signal was transmitted using a 500 kHz. Amplification and gradually attenuation is made in both AMCC and CPRI signals to change the ratio between the signals peak-to-peak voltage. We note that, all the published work is experimental, in this dissertation we develop a simulation model able to study systematically the effect of the AMCC channel for different operational parameters when the optical transmitter consists of a DFB laser followed by a MZM.

Chapter 6

Simulation Model and Case study

An implementation of the proposed system was made and simulated in MATLAB® in order to analyze the performance of the respective system. The models of the scheme used in the program is described in this chapter, as well as the simulation results. The simulation setup is described in section 6.1, the simulation results and respective discussions are presented in section 6.2.

6.1 Simulation setup

The simulation scheme is composed by a block of input signal, an optical link and processing signal blocks as represented in figure 6.1. An optical carrier is launched on the optical link where the optical carrier is modulated by the MZM. Thereafter, the modulated signal is transmitted to the optical receiver through the fiber. The received signal is processed after the transmission and its corresponding recovered signals are analyzed to evaluate the performance of the system.

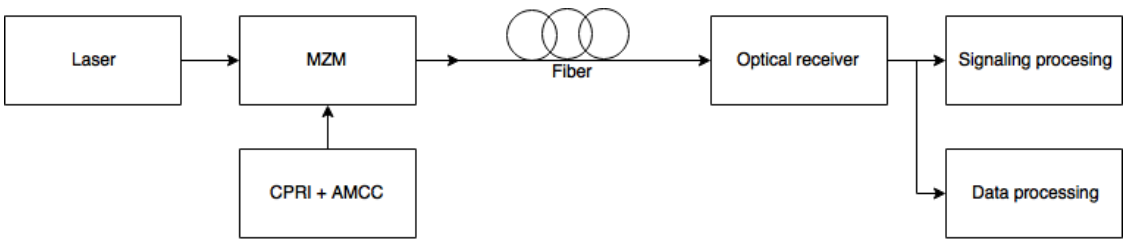

Figure 6.1: Overall system

6.1.1 CPRI + AMCC block

The input signal of this system corresponds to the signal resulting from the sum of CPRI data signal and AMCC signaling. The sum operation is performed in the block of input signal denominated CPRI + AMCC block. This block is composed by a CPRI data block and a AMCC signaling block as illustrated in figure 6.2.

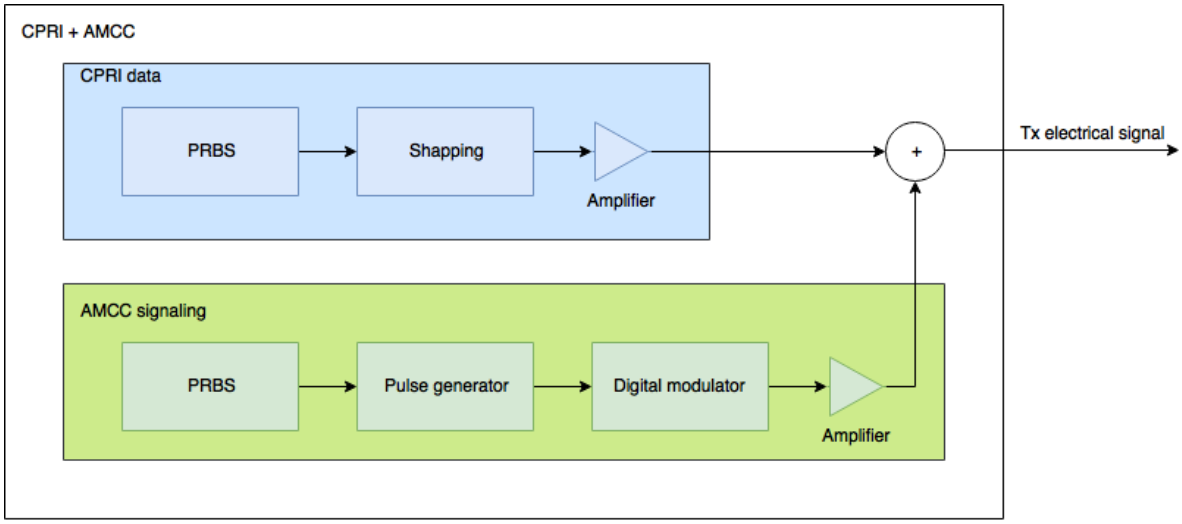

Figure 6.2: CPRI + AMCC block

The CPRI data block is the one responsible for CPRI data signal and it is constituted by a pseudorandom binary sequence (PRBS) generator, a transmitter filter, and an amplifier. The CPRI bit rate in this simulation was defined according to the table 4.1. The PRBS generator creates a pseudorandom CPRI bit sequence with -1 or 1 of amplitude. The *randi()* function is used to generate a sequence which amplitude's elements is 0 or 1. Then the amplitude is changed to -1 for bits whose amplitude is 0. The bit sequence generated is shaped by the transmitter filter which is a square-root raised cosine filter with a roll-off factor, β, equals to 0.25. This filter together with the filter at the receiver in data processing block, which employs the same square-root raised cosine filter, they combine a raised cosine filter which allow minimal intersymbol interference (ISI). After being filtered the signal is amplified by an amplifier whose function is to adjust the maximum and minimum values of the signal. The maximum amplitude allowed for the signal is $0.9 \times V_\pi$, where V_π is the switching voltage of the MZM. The amplifier gain for this simulation was set at 0.45.

Another point to consider in this stage is the λ-factor, which is responsible for managing the compromise between the amplitudes of CPRI data signal and AMCC signaling. The

λ-factor ensures these signals are operating outside the non-linear zone of MZM transfer curve and defines the amplitude of each signal aiming at the operation point where neither of the two signals degrade too much each other. For λ-factor equal to 0.5 the amplitude of CPRI and AMCC are equal but when you increase the λ-factor CPRI amplitude decreases and, consequently, AMCC amplitude increases. The λ-factor for this simulation was set at 0.2. With the amplification done the signal is passed for the next block where it will be summed with the AMCC signaling. Figure 6.3 and figure 6.4, illustrate the signals involved in each stage of AMCC data block with CPRI bit rate defined at 10.1376 Gbps.

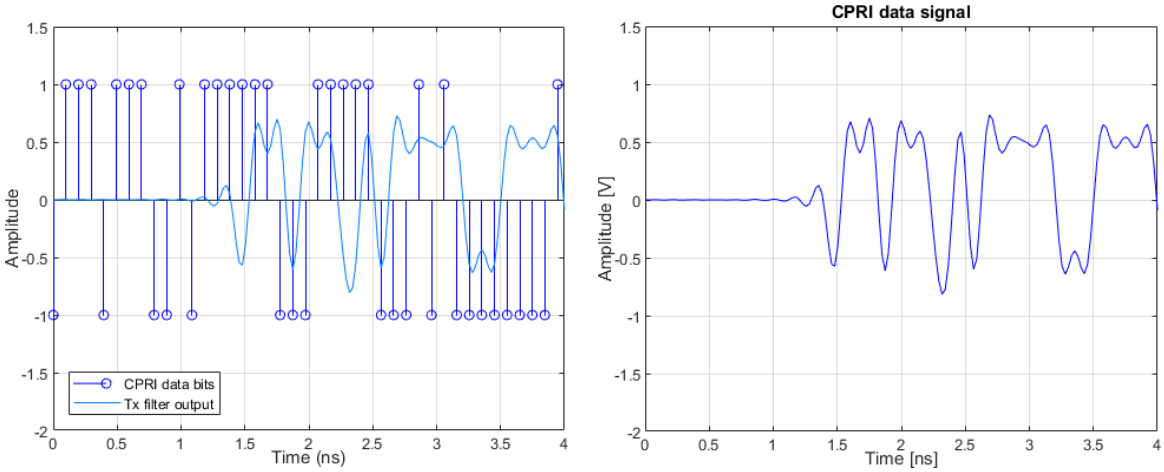

Figure 6.3: On the left are CPRI data bits and the correspondent output Tx filter. On the right is the resultant amplified signal

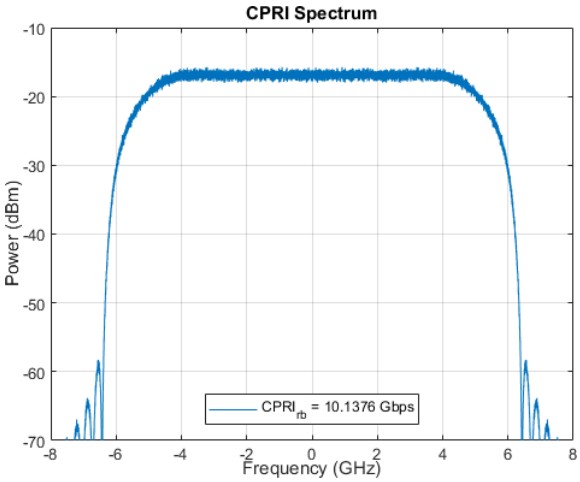

Figure 6.4: CPRI spectrum with $10,1376$ Gbps and $\beta = 0.25$

As a matter of visualization, the figures of the descriptions relating to the AMCC block will be merely illustrative since the bit rate of the CPRI used is not the actual rate, 10 Mbps. This is because the CPRI bit rates are much higher than the AMCC bit rates.

In other words, there are many CPRI data bits for a few AMCC signaling bits. For one signaling bit there is 1712 data bits as shown in figure 6.5, where CPRI and AMCC signaling data bit rate is 10.1376 Gbps and 200 kbps respectively.

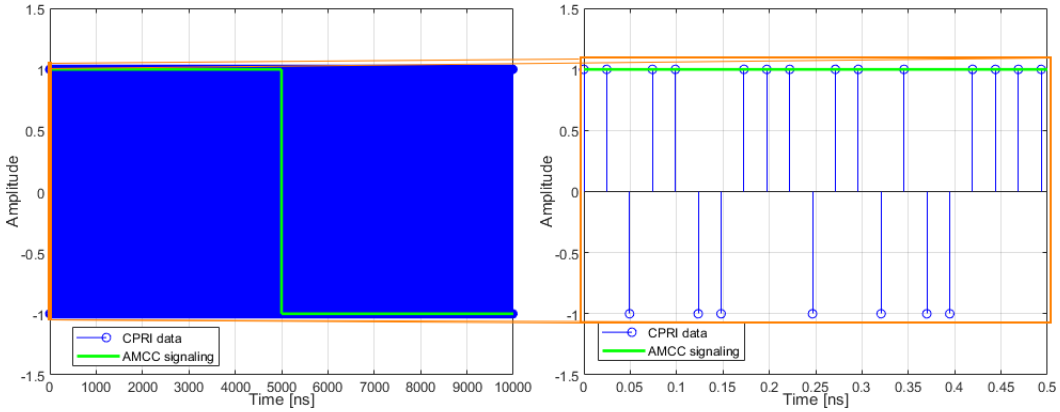

Figure 6.5: There are many CPRI data bits for a few AMCC signaling bits

The AMCC signaling is generated by four steps as we can see in figure 6.2. The PRBS block has identical function as the one in CPRI data block. It generates a bit sequence with elements which amplitude is -1 or 1. Then, it is necessary to form pulses corresponding of each signaling bit generated. This operation is executed in the Pulse generator block by a *rect()* function. The next step is digital modulation of the generated signal. The idea is the AMCC signal to be as simple and cheap as possible. Therefore, the modulation used in this work is Binary Phase Shift Keying (BPSK). However, other modulations may be used as indicated in article [25], provided these modulations are simple modulations. The modulation consists of the multiplication of the sequence of pulses with the modulation carrier $p(t) = cos(2\pi.f_{tone}.t_{simulation})$ where F_{tone} is the frequency of PT and $t_{simulation}$ is the simulation time. The last step is the amplification of the signal. As mentioned above, the amplitude must be equal to or less than $0.9 \times V_{\pi}$, and dependent on λ-factor. The frequency tone of the AMCC signaling was set in 1 MHz and simulations were carried out for AMCC bit rates, S_{rb}, equal to 200 kbps and 500 kbps. An example of the signals involved in this block are represented in figure 6.6 and figure 6.7 for AMCC bit rate set to 200 kbps.

With CPRI data signal and AMCC signaling set up it is time to add these two signals in the plus block and launch it into the optical link. An example of the resulting electrical transmitted signal is shown in figure 6.8 and figure 6.9. It is to be remembered that the figures are merely illustrative to better visualize the signaling, the CPRI bit rate used was 10 Mbps.

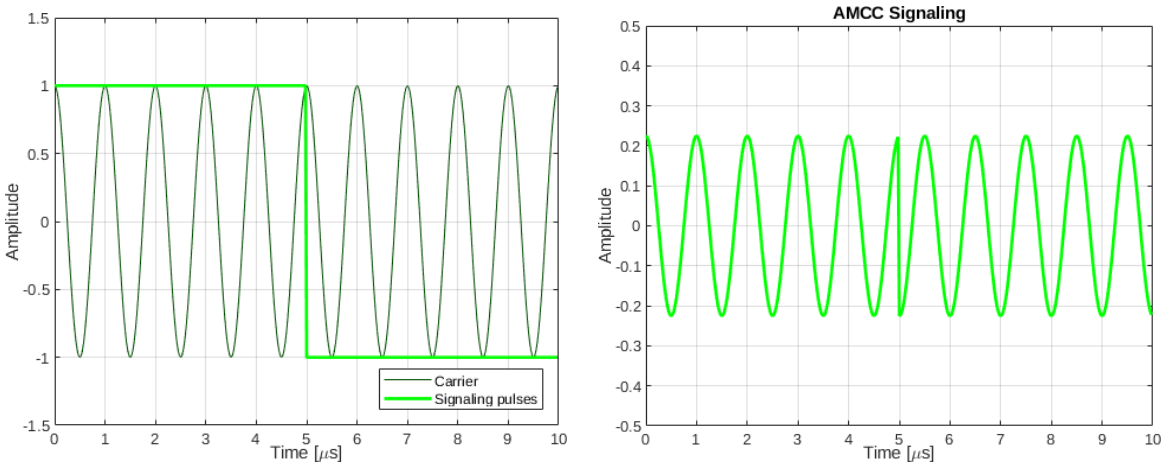

Figure 6.6: On the left are the previous pulses and modulation carrier, and on the right is the AMCC signaling modulated and amplified

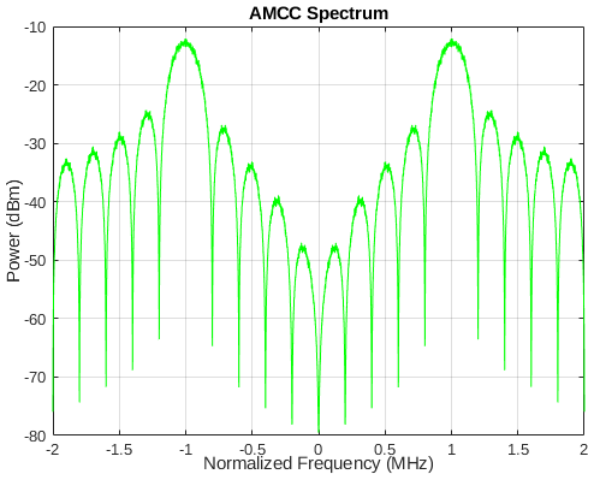

Figure 6.7: AMCC signaling spectrum with $f_c = 1$ MHz and $S_{rb} = 200$ kbps

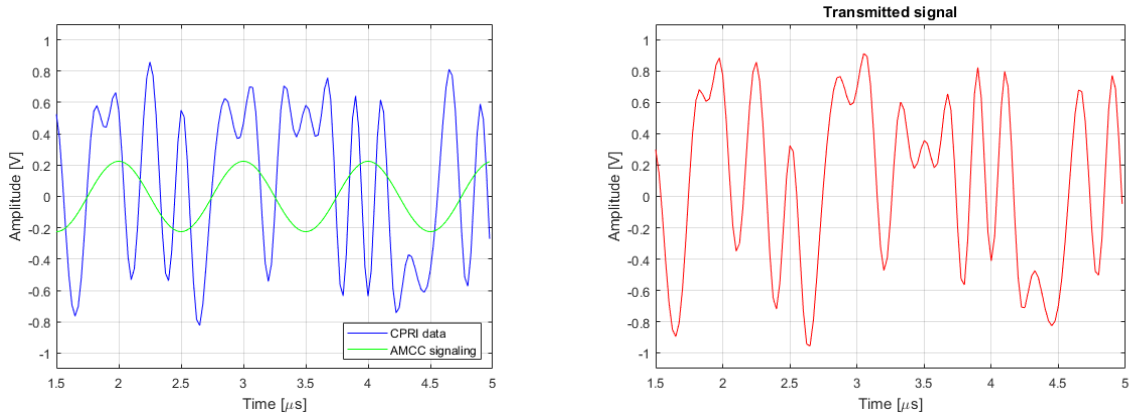

Figure 6.8: On the left is an illustrative figure of CPRI data and AMCC signaling. On the right is an illustrative figure of the transmitted signal

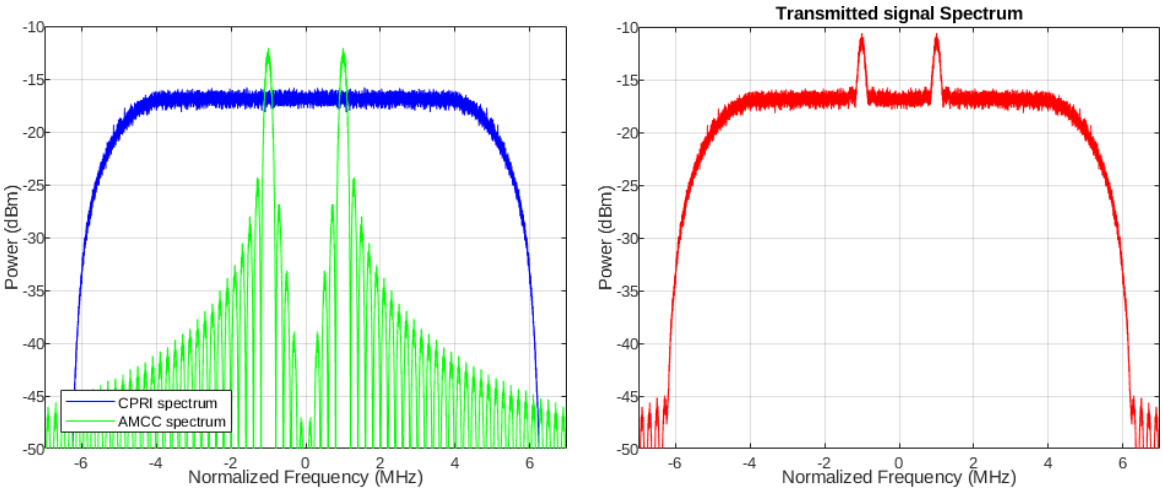

Figure 6.9: Illustrative figure of signals spectrums from the CPRI+AMCC block

6.1.2 Data and signaling processing

After transmission through the optical link the received signal is then directed to two different blocks to be analyzed: one block to process the CPRI data signal and the other block to process the AMCC signaling.

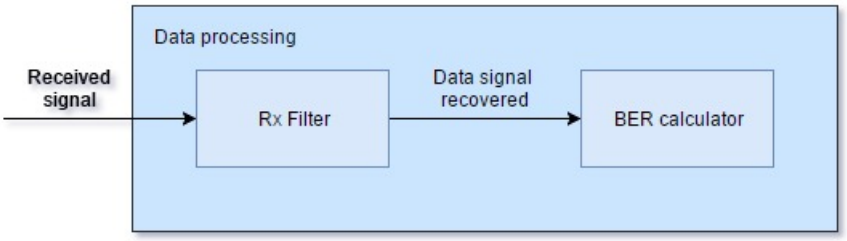

Figure 6.10: Data processing block

The data processing block is responsible for retrieving the CPRI data signal from the received signal of photodetector. The respective block is represented in figure 6.10. In data processing block the received signal is filtered by the receiver filter described above. In this case, the filter has a decimation factor and it is set at 1. As the transmitter filter adds points to the signal it is necessary to eliminate these additional points at this stage to be able to perform a correct processing. With these additional points eliminated, it is time to recover the CPRI data signal from the signal received. The *downsample()* function is used to pick up samples to return the CPRI data signal recovered. Once the CPRI data signal has been recovered it is send to the BER calculator to assess the impact of the AMCC. The BER calculation is done in the BER calculator which is described later. Illustrative examples of signals involved in this block are shown in figure 6.11 and figure 6.12. By the

opening of eye diagram, it can be concluded that the introduction of AMCC signaling had little degrading impact on the CPRI signal.

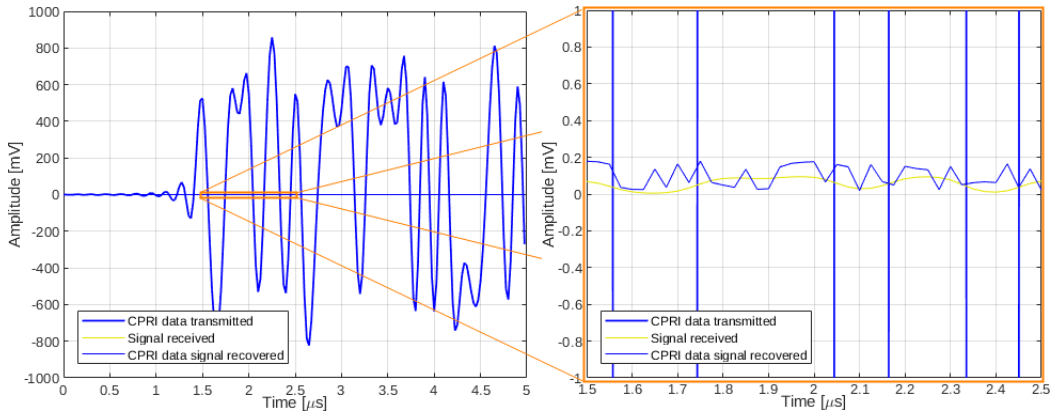

Figure 6.11: On the left is an illustrative figure of transmitted, received and recovered CPRI signals. On the right is a zoom on the illustrative figure.

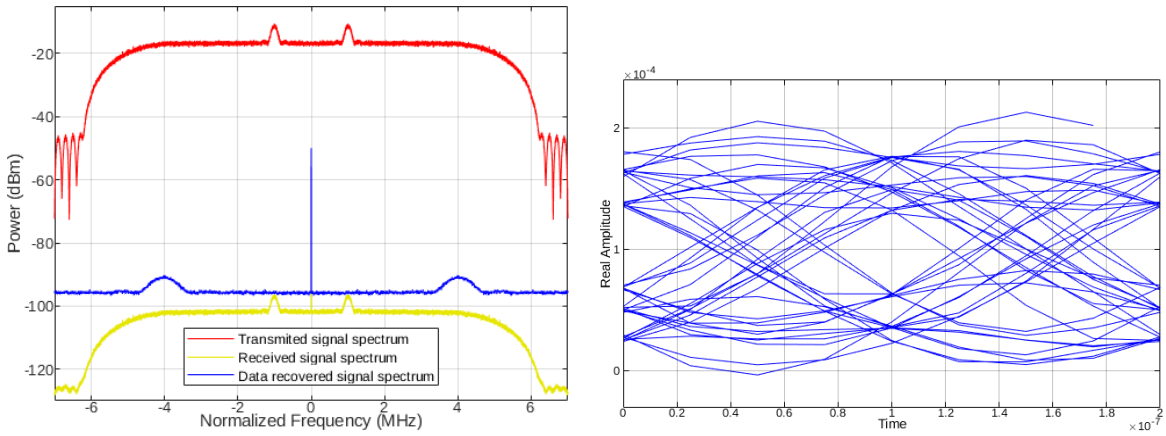

Figure 6.12: On the left, illustrative figure of transmitted, received and recovered CPRI signals spectrum. On the right is the CPRI signal eye diagram

On the other hand, the signaling processing block is responsible for retrieving the AMCC signaling from the received signal of photodetector. In signaling processing block, the received signal passes through two stages before to been recovered as AMCC signaling as shown in figure 6.13. The first step is demodulation which is done by multiplying the received signal by a carrier equal to the carrier applied in the modulation stage. Then the demodulated signal is filtrated. As the elemental pulse of AMCC signaling is rectangular the filter implemented in this system is an Integrated and Dump filter. After the filtration, the signaling is recovered and then it is send to BER calculator for recovery analyzes.

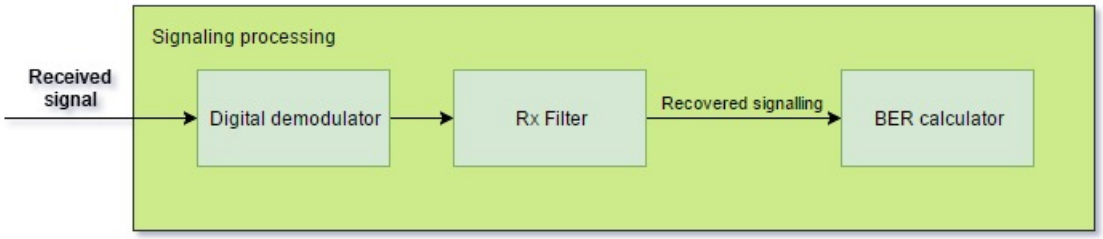

Figure 6.13: Signaling processing block

6.1.3 Bit Error Rate calculator

The objective of this case study is to know how feasible the proposed system is, and one way to analyze its performance is to calculate the BER of the recovered signals, CPRI data signal recovered and AMCC signaling recovered. It is possible to calculate BER by its definition and by a semi-analytic calculation. By definition BER is the number of bit errors in a transmitted bit sequence and it is given by equation (6.1).

$$BER = \frac{\text{number of wrong bits transmited}}{\text{total number of bits transmited}} \tag{6.1}$$

However, this option is impractical because the BER calculation is based on the bitwise comparison of the transmitted and recovered vectors. Usually, the bit sequence contains about 10^6 elements or more, which are quite a few bits and would cause the program to crash. An example of a BER model based in this option is represented in figure 6.14.

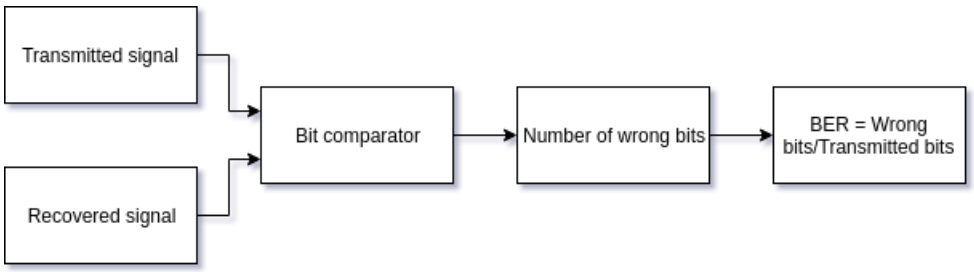

Figure 6.14: BER Calculator option 1

The semi-analytic BER calculation is presented in [26] and it is based on the Q parameter which is given by equation (6.2) where I_1 and I_0 are the average values relative to bit 1 and bit 0 respectively in the bit sequence, and σ_0 and σ_1 are their correspondent

standard deviation.

$$Q = \frac{I_1 - I_0}{\sigma_1 + \sigma_0} \tag{6.2}$$

With the Q parameter defined, the BER can be obtain by equation (6.3) where *erfc()* corresponds to the Complementary Error Function. This option was the one implemented in this simulation to calculate BERs of the recovered signals as *BER_calculator()* function. Since the values differ from iteration to iteration the BER will be the average of several iterations. The semi-analytic BER calculator model is represented in figure 6.15.

$$BER = \frac{1}{2} erfc(\frac{Q}{\sqrt{2}}) \tag{6.3}$$

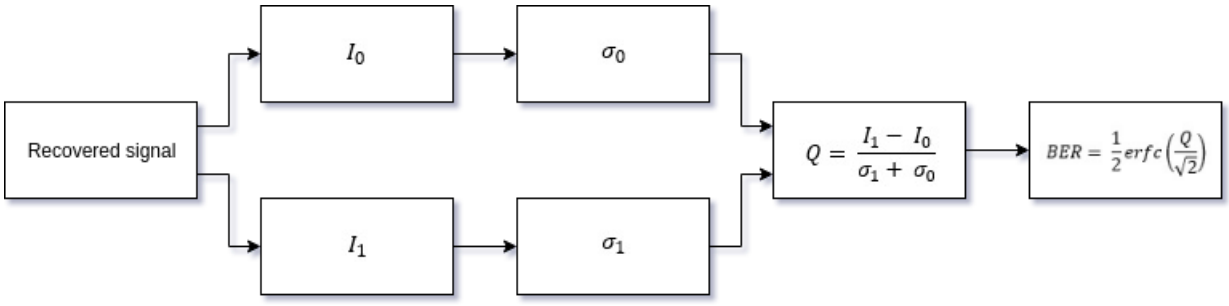

Figure 6.15: Semi-analytic BER calculation

6.1.4 Optical link

The optical link shown in figure 6.1 is constituted by an optical transmitter which is connected to an optical receiver through a single mode fiber (SMF). The optical transmitter uses a Laser and MZM as optical source and for optical modulation, respectively.

In this simulation it is used *lasercw(t,powerdBm,initPhase,linewidth,varargin)* function, which was developed in the scope of a PhD thesis [27], as a continuous wave laser model.

The input parameters used in this simulation are 1 MHz for linewidth and a variable power dependent in which tests are carried out. The optical carrier works at 1550 nm wavelength.

The model for the MZM was implemented according to [28]. It was used a dual-drive MZM and according to [29] the transmitted optical field $E_{MZM}(t)$ by the MZM is given by equation (6.4), where E_{laser} is the electrical field of the laser, "V_π is the switching voltage required to create a π phase shift on the light wave carrier and has typical values within a range of $2-6V$. $V(t)$ is a time-varying driving signal voltage. V_{bias} is a DC bias voltage which is normally coupled with the signal source using a T-bias device." In this simulation, $V(t)$ corresponds to the electrical transmitted signal resulting from the CPRI+AMCC block.

$$E_{MZM}(t) = E_{laser}\cos\left(\frac{\pi}{2}\frac{(V(t)+V_{bias})}{V_\pi}\right) \tag{6.4}$$

The MZM is polarized at the quadrature point, $V_{bias} = \frac{V_\pi}{2}$, so it is possible to work in the linear zone of the MZM's transfer characteristic as we can see in figure 6.16. The MZM model is performed by *dd_mzm()* function which implements the equation (6.4). Considering that the objective is to work in the linear zone of the transfer curve of MZM, observing the respective curve, we conclude why the λ-factor and the gain of the amplifier used in this simulation are respectively 0.2 and 0.45.

As said above, the optical fiber channel is a SMF and its behavior is performed by the $E_{fiber} = smf(t, E_{MZM}, L)$ function which implements the linear transfer function model for purely dispersive SMF with 0.22 dB/km of attenuation and 16 ps/km/nm of dispersion. However, in calculating the frequency response of the fiber the attenuation was canceled in order to allow the $smf()$ function to be independent of the change in fiber length. That is, by canceling the attenuation in the *smf()* function it is no longer necessary to adjust the input power on the fiber whenever the fiber length is changed. Thus, by trial and error the power of the laser was adjusted so that the power received could provide a BER close to the BERs calculated experimentally in the referenced articles, that is $BER = 10^{-9}$ for -20dBm.

Normally, the optical receiver is composed of a photodetector, a filter, and a decision circuit as we can see in figure 6.17. However, the optical receiver used in this work consists

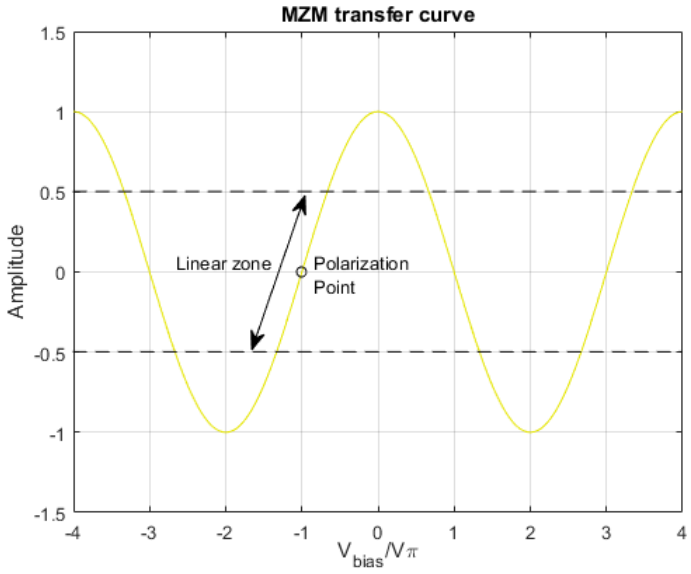

Figure 6.16: Transfer characteristics of MZM

only of the photodetector. The reason for this implementation is that the processing of the signals is done from the average of the bits corresponding to the recovered signal as explained above and it is not necessary to use bits in this processing.

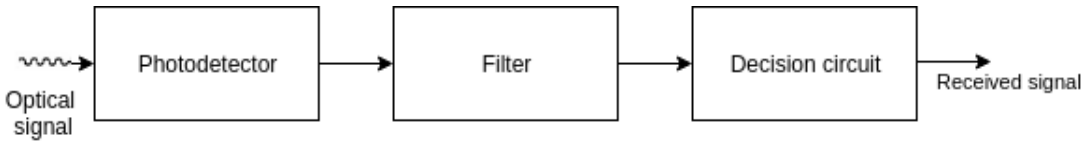

Figure 6.17: Optic Receiver

Thus, the optical receiver of this simulation consists only of the photodetector. The photodetector receives the incident optical power from the optical fiber channel and converts it into the correspondent photocurrent I_p which, according to [26], is given by equation (6.5), where R is the responsivity of the photodetector and P_{in} is the incident optical power. The responsivity is in units of A/W and it was set at 1 A/W to allow maximum quantum efficiency.

$$I_p = RP_{in} \tag{6.5}$$

The incident optical power is in units of W and it is given by equation (6.6), where E_{fiber} is the fiber electro field.

$$P_{in} = |E_{fiber}|^2 \tag{6.6}$$

The photodetector introduces noises with thermal noise being the most relevant one. Thus, a noise whose power spectral density is 1.93×10^{-11} A/Hz was added to the photocurrent. To conclude this description figure 6.18 illustrates all the models implemented in the simulation of this case study.

6.2 Simulation results and discussion

In this section we evaluate the effect of the parameters that characterize the system itself, such as λ-factor, CPRI data signal bit rate, AMCC signaling bit rate, and fiber length. To do that, tests were carried out where these parameters were varied and the BER was calculated. According to reference [29], a good response to the system is when BER is less than 10^{-3}. Therefore, FEC limit for this simulation was defined to $BER = 10^{-3}$. The CPRI data bit rates used in the simulation was 2.4576 Gbps, 4.9152 GBPS and 10.1376 Gbps. The AMCC signaling CPRI data bit rates used in the simulation was 200 kbps and 500 kbps with a carrier frequency of 1 MHz.

The first case to be studied was how the CPRI data signal behaves with the variation of received power. With defined fiber length at 0 km the CPRI data BER was calculated for the three CPRI bit rates according to the received power variation. It should be noted that in this study the λ-factor was not used since the study signal was CPRI data. The λ-factor is used only when there is the sum of the CPRI data signal with the AMCC signaling. The resulting graph of the simulation is shown in figure 6.19. It is observed that for all CPRI data bit rate in study the system works well for received power above -24 dBm.

As for AMCC signaling, a study was carried out to determine the impact of the λ-factor on AMCC signaling. With defined fiber length at 0 km and laser power fixed at -10 dBm, the AMCC signaling BER was calculated for the three CPRI bit rates according to the λ-factor variation for AMCC bit rates equal to 200 kbps and 500 kbps. The resulting graph of the simulation is shown in figure 6.20. As can be observed, BER increases with increasing λ-factor. The reason for this behavior is the fact that the signaling is directly proportional

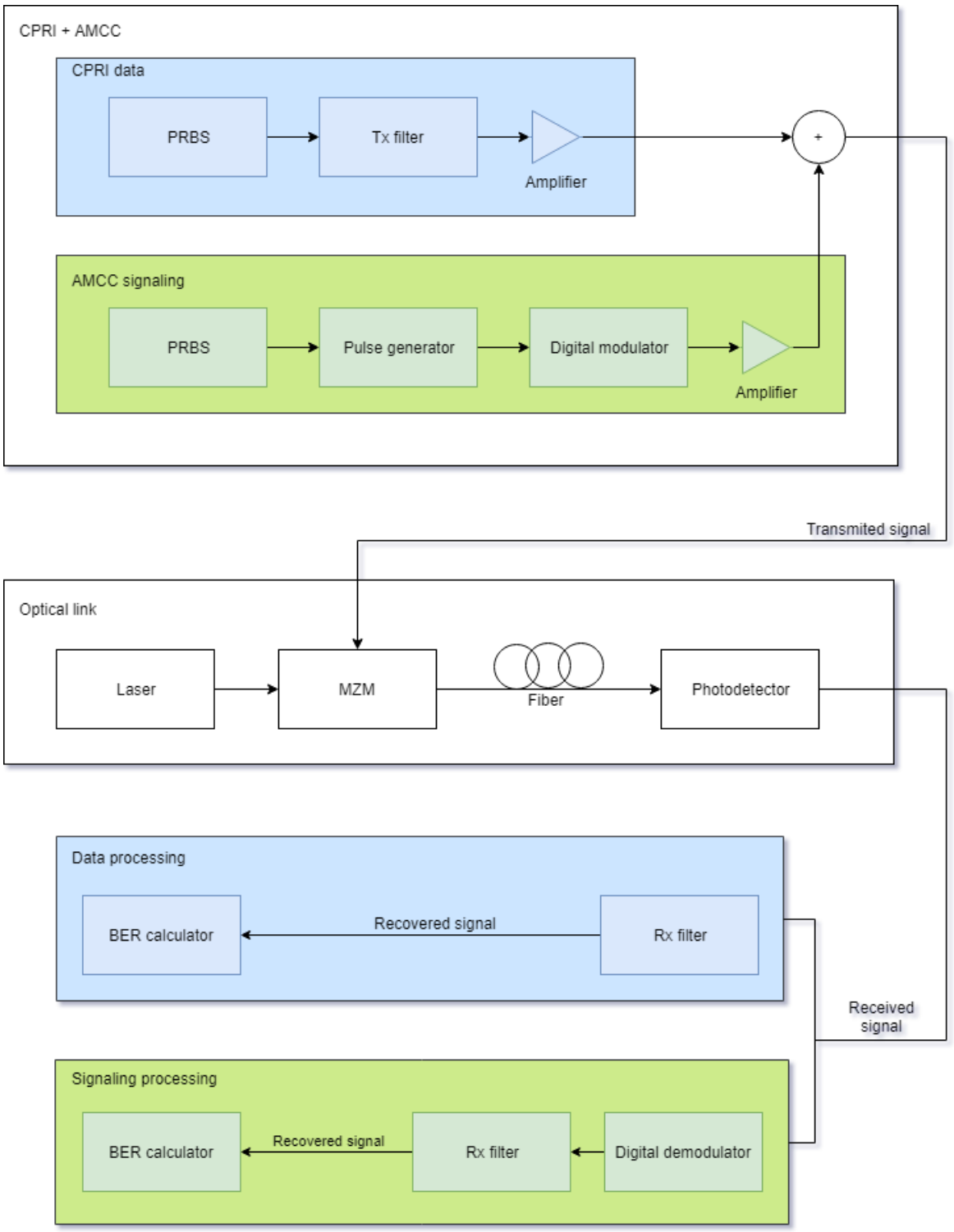

Figure 6.18: Simulation models

to the λ-factor: the higher the λ-factor the greater is the amplitude of the signaling. For AMCC signaling bit rate equals 200 kbps, the system works well for values greater than 0.035 for any of the CPRI data bit rates in study. And for AMCC signaling bit rate equals 500 kbps, the system works well for values greater than 0.004 for any of the CPRI data bit rates in study.

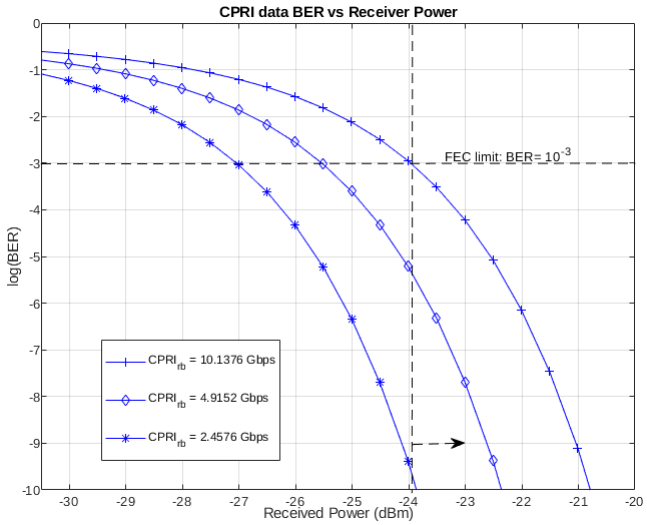

Figure 6.19: CPRI data BER vs Received Power

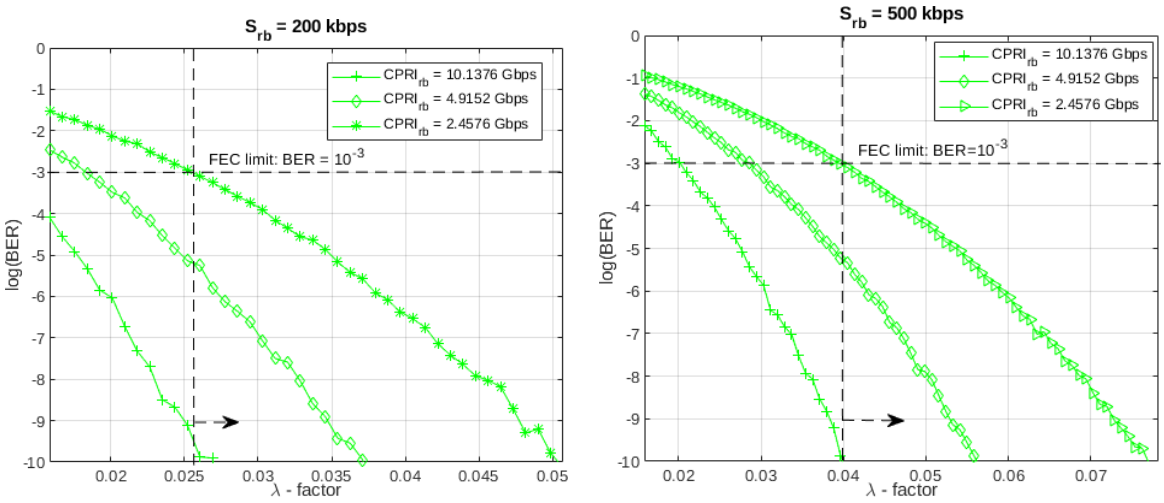

Figure 6.20: BER signaling vs λ-factor for $S_{rb} = 200$ kbps on the left side and for $S_{rb} = 500$ kbps on the rigth side

On the other hand, to determine the impact of the λ-factor on CPRI data signal a study was carried out with fiber length defined at 0 km and laser power fixed at -10 dBm. The CPRI data BER was calculated for the three CPRI data bit rates according to the λ-factor variation for AMCC signaling bit rates equals to 200 kbps and 500 kbps. The resulting graph can be seen in figure 6.21 and figure 6.22. It verifies that the CPRI data BER decreases with the increase of the λ-factor. This is because CPRI data is inversely proportional to the λ-factor: the higher the λ-factor the smaller is the amplitude of the CPRI data signal. It is noted that the AMCC signaling bit rates used do not degrade the signal since the graphics are similar for both 200 kbps and 500 kbps. It is also noted that there is no difference in behavior between the graphs referring to the CPRI data bit rates used. Therefore, the system works well for λ-factor less than 0.217 for all CPRI data bit rates used.

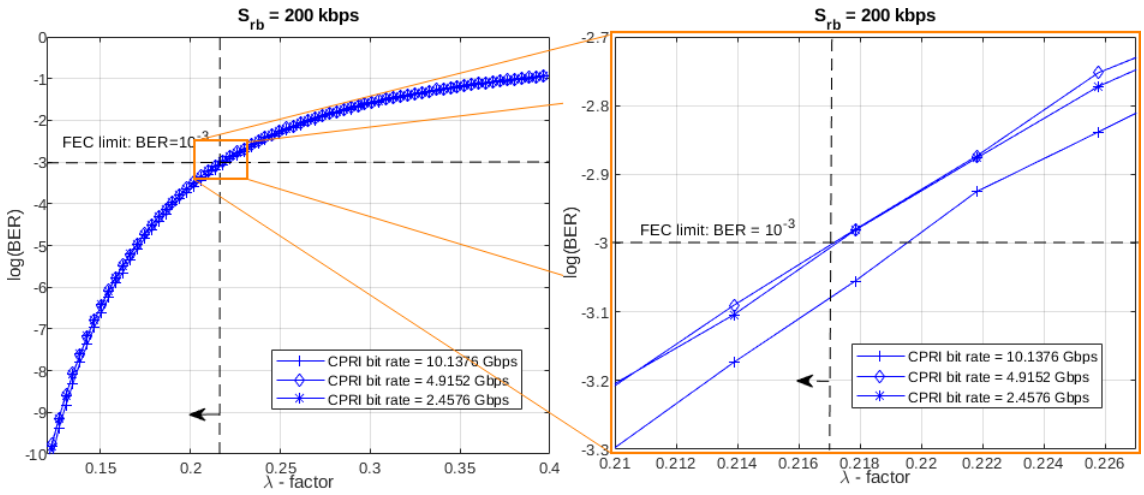

Figure 6.21: CPRI data BER vs λ-factor for AMCC bit rate = 200 kbps

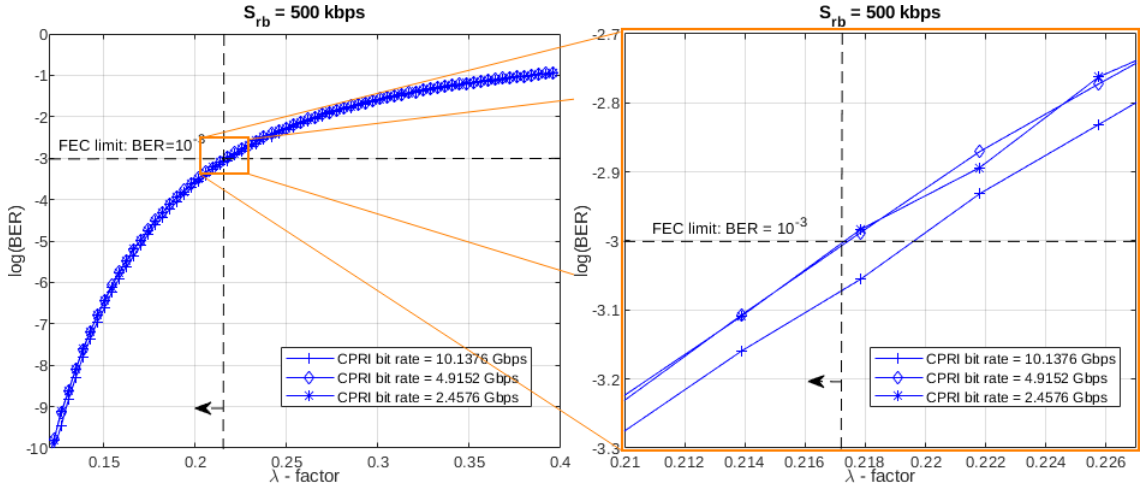

Figure 6.22: CPRI data BER vs λ-factor for AMCC bit rate = 500 kbps

Analyzing the results of the two previous studies about BER response according to the λ-factor, we conclude that for the defined fiber length at 0 km, laser power fixed at -10 dBm, AMCC signaling bit rate at 200 kbps or 500 kbps, and CPRI data signal bit rate at 2.4576 Gbps, 4.9152 Gbps or 10.1376 Gbps, the λ-factor to be used must be in the range of 0.035 to 0.217 as illustrated in figure 6.23.

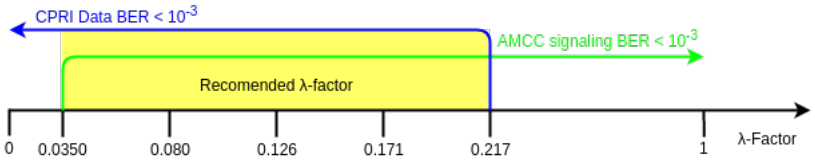

Figure 6.23: λ-factor margin

To determine the impact of the fiber length on CPRI data signal a study was carried out with laser power fixed at -10 dBm and fiber length varied from 0 km to 80 km. Figure 6.24

to figure 6.26 show the results from the simulation. It is observed that the fiber length variation has little or no influence on the performance of the system with 2.4576 Gbps and 4.9152 Gbps CPRI bit rates. Since the graphs of different fiber lengths overlap each other with both AMCC bit rates at 200 kbps and at 500 kbps. In this scenario, the system works well for λ-factor less than 0.217 for CPRI data signal bit rates of 2.4576 Gbps and 4.9152 Gbps.

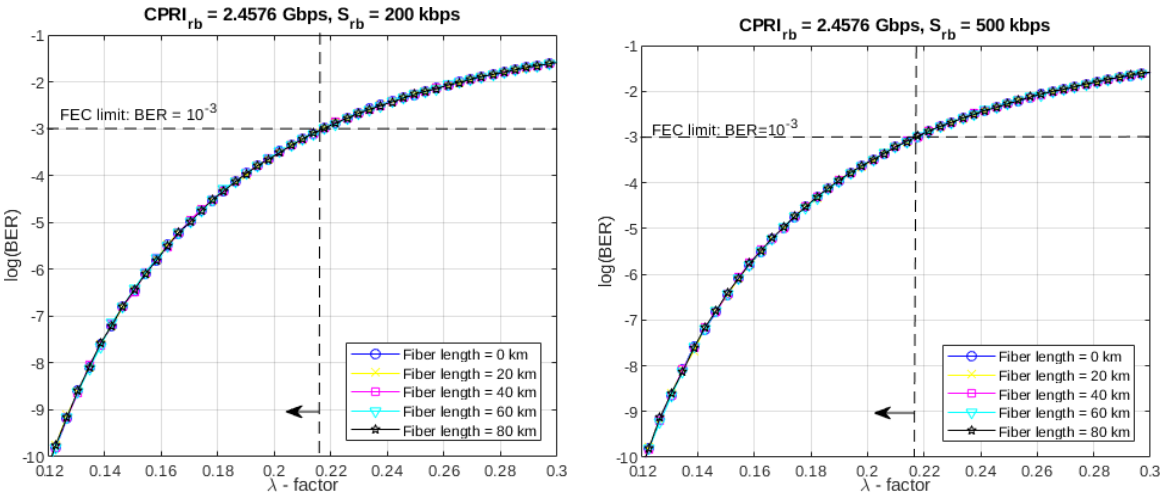

Figure 6.24: BER data vs λ-factor for 2.4576 Gbps with $S_{rb} = 200$ kbps on the left side and with $S_{rb} = 500$ kbps on the rigth side

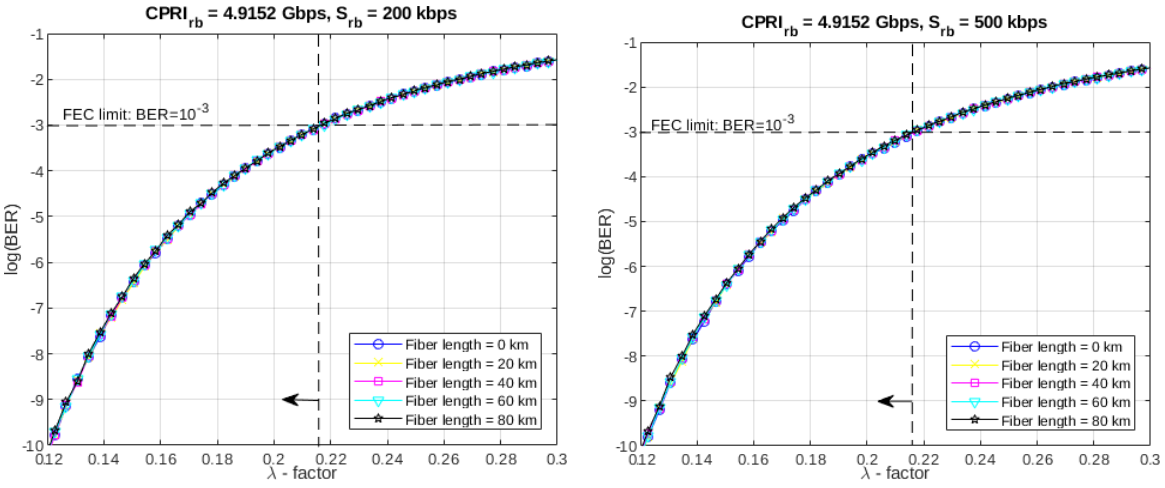

Figure 6.25: BER data vs λ-factor for 4.9152 Gbps with $S_{rb} = 200$ kbps on the left side and with $S_{rb} = 500$ kbps on the rigth side

However, there is a difference of behavior in the graphics referring to the CPRI data bit rate at 10.1376 Gbps. For fiber lengths of 0 km, 20 km, and 40 km the behavior of the CPRI data BER is practically similar with slight differences. While for the 60 km and 80 km wavelengths, there is already a deviation from the behavior of BER compared to the

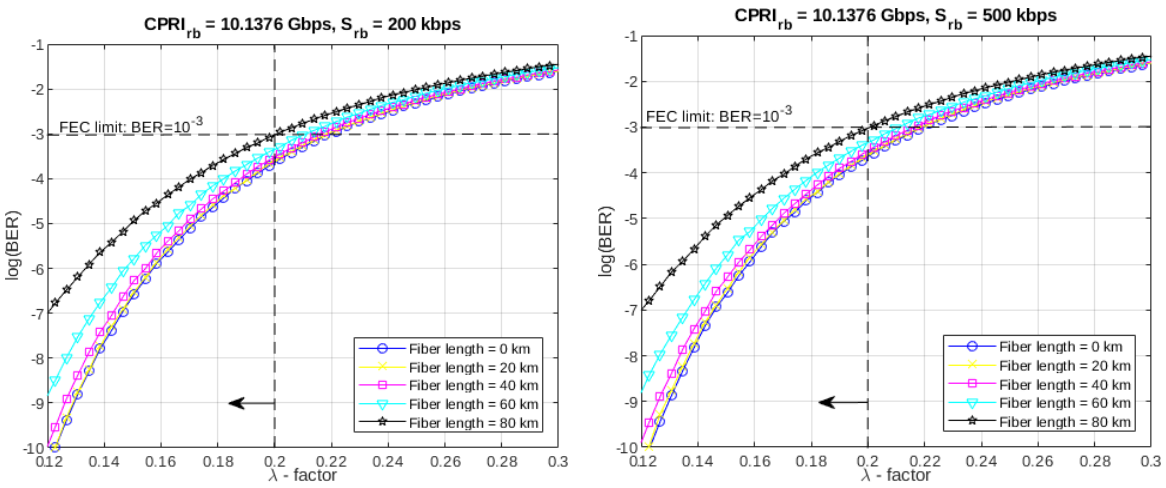

Figure 6.26: CPRI data BER vs λ-factor for 10.1376 Gbps with $S_{rb} = 200$ kbps on the left side and with $S_{rb} = 500$ kbps on the rigth side

others which indicates a degradation in the signal that can be seen by the decrease of the BER. Such behavior was to be expected since the larger the fiber length the greater the attenuation loss and consequently the worse the signal being transmitted. Therefore, for CPRI data bit rate equals to 10.1376 Gbps the system works well for λ-factor less than 0.2 for fiber length from 0 km to 80 km, as shown in figure 6.27.

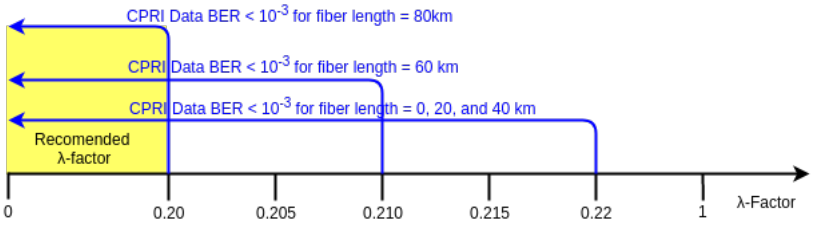

Figure 6.27: λ-factor dimensioning for CPRI data bit rate equals to 10.1376 Gbps and fiber length from 0 km to 80 km

The objective of this case study is to know how feasible the proposed system is, that is, to analyze the possibility of introducing AMCC signaling as a PT form in CPRI data signal with the lowest CPRI data signal degradation possible. For that, simulations for the case study were made and the results obtained were satisfactory. Table 6.1 summarizes the simulation results from the four studies performed considering the limiting FEC defined as being $BER = 10^{-3}$: CPRI data BER vs Received Power, BER signaling vs λ-factor, CPRI data BER vs λ-factor, and CPRI data BER vs λ-factor. The first line of the table corresponds to the parameters that characterize the system which were varied for each study.

	CPRI data bit rate (Gbps)	AMCC signaling bit rate (kbps)	λ-factor	Received power (dBm)	Fiber length (km)
BER signaling vs λ-factor	2.4576	———-	0.2	-27	0
	4.9152			-25.5	
	10.1376			24	
BER signaling vs λ-factor	2.4576	200	0.0158	-10	
	4.9152		0.025		
	10.1376		0.035		
	2.4576	500			
	4.9152				
	10.1376				
CPRI data BER vs λ-factor	2.4576	200 500	0.217		
	4.9152		0.217		
	10.1376		0.219		
CPRI data BER vs λ-factor	2.4576	200 500	0.217		0, 20, 40, 60 and 80
	4.9152		0.217		
	10.1376		0.22		0
			0.219		20
			0.218		40
			0.21		60
			0.2		80

Table 6.1: Simulation results resume

Chapter 7

Conclusion

This chapter presents the overall dissertation conclusions and future work. The principal conclusions are presented in section 7.1 and some possible future works suggestions are discussed in section 7.2.

7.1 Conclusions

With the objective of study the integration and support of the 5G mobile network through the access network NG-PON2, a study of NG-PON2, particularly the mobile network support mechanisms, was carried out in a first phase. It was stated that the 40-Gigabit-capable passive optical networks, the NG-PON2, standardized in ITU-T G.989 series [12] is suitable to fulfill the high demands of bandwidth. Through its PtP WDM technology and wavelength tunability the operators can offer good quality access services with a reduced number of resources and infrastructures. With its management and information functions, AMCC boosts the network.

Secondly, a study of C-RAN architectures and CPRI was discussed. The big advantages of C-RAN are its centralization and pooling of resources between BBUs and sharing connections between several BBUs and RRHs. The constant bit rate interface CPRI provides sufficient bit rate to transmit the several LTE signals existent and the physic layer of CPRI could be implemented in fiber which means that CPRI is suitable for adapt C-RAN to NG-PON2.

Thirdly, real implementations of the AMCC RF PT approach were studied, and all of them confirmed the feasibility of the proposed system. Finally, a simulation model from

MATLAB® was developed and tested with focus on the analysis of the effect of the AMCC on the transmission of CPRI signals from the mobile network. The results follow the conclusion of the real implementation study before and with all the study carried out, it was concluded that the approach of converging the C-RAN architecture with the NG-PON2 access network implementing PtP WDM PON with the AMCC is feasible and promisor.

7.2 Future Work

The network discussed in this dissertation meets the current demands of both consumer and telecom operator. However, there are several parameters which researchers can explore to complement or even upgrade the respective network. As we saw, this network is still open to development and it requires future improvements, so the network can keep up with the bandwidth demand and with other issues which definitely will emerged over the next few years.

I have no concrete idea of a future work regarding to the proposed network. However, I leave here some questions that could lead to a pilot idea of a possible project. About the network itself, will the network be prepared for cyber-attacks? To what extent are exterior components protected by environmental factors? To what extent are the network components reliable? As for the system parameters, I start with NG-PON2: What is the most efficient way to adapt the OLT and the BBUs and the ONU and the corresponding RRH? What ensures that ODN components have negligible degradation in fronthaul? Will there be other, more efficient ways to implement AMCC? Regarding to C-RAN, will CPRI be the best interface to be implemented for fronthaul? What is the distance to be considered "error free" between RRH and BBU? How to efficiently adapt the various BBUs in a system of sharing of resources and infrastructures?

Researchers as C. Wagner and his team present in [30] a "comparative analysis of resilience of wavelength-selective and wavelength-routed architectures against crosstalk attackers", L. Anet Neto and his team in [31] experimentally assessed compression with scalar and vector quantization for fixed-mobile convergent networks, and Marco Ruffini discusses in [32] "a new vision requires dealing with network convergence at a multi-dimensional level." And with this study he identified many open areas of research, which he believes that it will become increasingly relevant in the coming years.

Bibliography

[1] Eurostat, "Information and Communication Technologies usage in households and by individuals," *European Journal of Humour Research*, 2016.

[2] Cisco Mobile, *Cisco Visual Networking Index: Global Mobile Data Traffic Forecast Update, 2016-2021 White Paper*, 2017.

[3] S. Gosselin, A. Pizzinat, X. Grall, D. Breuer, E. Bogenfeld, S. Krauß, J. A. T. Gijón, A. Hamidian, N. Fonseca, and B. Skubic, "Fixed and Mobile Convergence: Which Role for Optical Networks?" *Journal of Optical Communications and Networking*, vol. 7, no. 11, p. 1075, 2015. [Online]. Available: https://www.osapublishing.org/abstract.cfm?URI=jocn-7-11-1075

[4] ITU-T, "ITU-T Recommendation G.984.2 - 40-Gigabit-capable passive optical networks 2 (NG-PON2): Physical media dependent (PMD) layer specification," 2014.

[5] M. Peng, Y. Sun, X. Li, Z. Mao, and C. Wang, "Recent Advances in Cloud Radio Access Networks: System Architectures, Key Techniques, and Open Issues," *IEEE Communications Surveys & Tutorials*, vol. PP, no. 99, pp. 1–1, 2016. [Online]. Available: http://ieeexplore.ieee.org/lpdocs/epic03/wrapper.htm?arnumber=7444125

[6] N. C. A. L. Ericsson AB, Huawei Technologies and N. Networks, "Common public radio interface (CPRI); interface specification v7.0," *Huawei Technologies Co. Ltd, NEC Corporation, Alcatel Lucent, and Nokia Networks*, 2015.

[7] A. de la Oliva, J. A. Hernández, D. Larrabeiti, and A. Azcorra, "An overview of the CPRI specification and its application to C-RAN-based LTE scenarios," *IEEE Communications Magazine*, vol. 54, no. 2, pp. 152–159, 2016.

[8] J. Dong and J. Yang, "Cascaded Phase Modulation for AMCC Superimposition Toward MFH Employing CPRI," *IEEE Photonics Journal*, vol. 9, no. 4, 2017.

[9] P. C. Zakaria Tayq, Luiz Anet Neto and C. Aupetit-Berthelemot, "Experimental real time AMCC implementation for fronthaul in PtP WDM-PON," pp. 1–3, 2016.

[10] N. Ansari and J. Zhang, *Media access control and resource allocation: For next generation passive optical networks*. Springer Science & Business Media, 2013.

[11] A. Abdalla, "Next-generation broadband optical access technologies for extensible heterogeneous radio architectures," Ph.D. dissertation, 9 2014.

[12] International Telecommunication Union. Transmission systems and media, digital systems and networks. [Online]. Available: http://www.itu.int/rec/T-REC-G/en

[13] 3GPP. Releases. [Online]. Available: http://www.3gpp.org/specifications/releases

[14] ITU-T, "ITU-T Recommendation G.989.3 - 40-Gigabit-capable passive optical networks (NG-PON2): Transmission Convergence Layer Specification," 2015.

[15] D. A. Khotimsky, "NG-PON2 Transmission Convergence Layer: A Tutorial," *Journal of Lightwave Technology*, vol. 34, no. 5, pp. 1424–1432, 2016.

[16] ITU-T, "ITU-T Recommendation G.989.2 Amendment 2 - 40-Gigabit-capable passive optical networks 2 (NG-PON2): Physical media dependent (PMD) layer specification Amendment 2," 2017.

[17] H. Zarrinkoub, *Understanding LTE with MATLAB: From Mathematical Modeling to Simulation and Prototyping*. John Wiley & Sons, 2014.

[18] A. Pizzinat, P. Chanclou, F. Saliou, and T. Diallo, "Things You Should Know About Fronthaul," *Journal of Lightwave Technology*, vol. 33, no. 5, pp. 1077–1083, 2015.

[19] Viavi Solutions Inc, "Radio Frequency Analysis at Fiber-Based Cell Sites," 2015.

[20] T. Pfeiffer, "Next Generation Mobile Fronthaul and Midhaul Architectures," *IEEE/OSA Journal of Optical Communications and Networking*, vol. 7, no. 11, pp. B38–B45, 2015.

[21] S. Kaneko, T. Yoshida, and K. Asaka, "In-Service Wavelength Tuning Technology in WDM/TDM-PONs for Multiple-Service Convergence," in *ECOC 2015; 41st European Conference on Optical Communication*, 2015, pp. 1–3.

[22] G. Nakagawa, K. Sone, S. Oda, S. Yoshida, Y. Aoki, M. Takizawa, and J. C. Rasmussen, "Experimental Investigation of AMCC Superimposition Impact on CPRI Signal Transmission in DWDM-PON Network," in *ECOC 2016; 42nd European Conference on Optical Communication*, 2016, pp. 1–3.

[23] K. Honda, T. Kobayashi, T. Shimada, J. Terada, and A. Otaka, "WDM Passive Optical Network Managed with Embedded Pilot Tone for Mobile Fronthaul," in *ECOC 2015; 41st European Conference on Optical Communication*, 2015, pp. 1–3.

[24] K. Honda, T. Kobayashi, S. Nishihara, T. Shimada, J. Terada, and A. Otaka, "Experimental Analysis of LTE Signals in WDM-PON Managed by Embedded Pilot Tone," *IEEE Photonics Technology Letters*, vol. 29, no. 5, pp. 431–434, March 2017.

[25] M. H. Eiselt, C. Wagner, and M. Lawin, "Remotely Controllable WDM-PON Technology for Wireless Fronthaul/Backhaul Application," in *2016 21st OptoElectronics and Communications Conference (OECC) held jointly with 2016 International Conference on Photonics in Switching (PS)*, July 2016, pp. 1–3.

[26] G. P. Agrawal, *Fiber-Optic Communication Systems*, 3rd ed. John Wiley & Sons, 2002.

[27] P. A. F. d. Almeida, "Radio over Fiber Systems with Support for Wired and Wireless Services," Ph.D. dissertation, Universidade de Coimbra, July 2014. [Online]. Available: http://hdl.handle.net/10316/25263

[28] J. Terada, T. Shimada, T. Shimizu, and A. Otaka, "Optical Access Network Technology for 5G Wireless Front/Backhaul Network," in *2016 21st OptoElectronics and Communications Conference (OECC) held jointly with 2016 International Conference on Photonics in Switching (PS)*, July 2016, pp. 1–3.

[29] L. N. Binh, *Optical Fiber Communication Systems with Matlab® and Simulink® Models*, 2nd ed. CRC Press, 2014.

[30] C. Wagner, M. Eiselt, K. Grobe, J. L. Wei, J. J. Vegas Olmos, and I. Tafur Monroy, "Evaluation of Crosstalk Attacks in Access Networks," pp. 1–3, 2016.

[31] L. A. Neto, P. Chanclou, Z. Tayq, B. C. Zabada, F. Saliou, and G. Simon, "Experimental Investigation of Compression with Fixed-length Code Quantization for Convergent Access-Mobile Networks," in *ECOC 2016; 42nd European Conference on Optical Communication*, Sept 2016, pp. 1–3.

[32] M. Ruffini, "Multidimensional Convergence in Future 5G Networks," *Journal of Lightwave Technology*, vol. 35, no. 3, pp. 535–549, Feb 2017.